Planetary- and Synoptic-Scale Signatures Associated with Central American Cold Surges

DAVID M. SCHULTZ,* W. EDWARD BRACKEN, AND LANCE F. BOSART

Department of Earth and Atmospheric Sciences, University at Albany, State University of New York, Albany, New York

(Manuscript received 23 July 1996, in final form 27 March 1997)

ABSTRACT

Motivated by outstanding issues from a previous case study of a midlatitude cold surge that affected Mexico and Central America, the climatology of Central American cold surges is examined in this paper. An independently derived listing of 177 cold-surge events is employed for which the following properties are tabulated: onset date, duration, time between cold-surge events, latitude of maximum equatorward penetration (ϕ_{min}), and 48-h maximum surface temperature change at Merida, Mexico (ΔT). These data show that 75% of the cold surges have durations of 2–6 days, the same timescale as mobile disturbances in the westerlies. Also, there does not appear to be any relationship between ΔT and the duration of the event, although cold surges that penetrate to low latitudes (ϕ_{min} = 7°–10°N) have a weak tendency to persist longer than those that do not penetrate to low latitudes (ϕ_{min} = 15°–20°N). In addition, the Reding data indicate that the cold surges tend to reach their most equatorward extent where topographic features impede the progress of equatorward-moving cold air; the temperature decrease in the postsurge air (as measured by ΔT) does not appear to be related to the most equatorward extent.

To examine the planetary- and synoptic-scale patterns associated with different categories of cold surges, events with similar characteristics from this database were composited: COLD ($\phi_{min} \leq 10°$N and $\Delta T \geq 9°$C), COOL ($\phi_{min} \leq 10°$N and $\Delta T = 4°$–$5°$C), and LONG (events lasting at least 8 days). COLD surges are characterized by a persistent upper-level ridge over the western United States, 200-hPa confluence over the Gulf of Mexico, and the migration of a Canadian lower-tropospheric anticyclone equatorward along the Rocky Mountains and the Sierra Madre. In contrast, COOL surges are associated with a progressive, upper-level ridge over the western United States, weak 200-hPa confluence over the Gulf of Mexico, and the migration of a North Pacific anticyclone over the intermountain west and into the southeast United States. LONG surges are associated with a slower-moving planetary-scale pattern; 200-hPa confluence over the Gulf of Mexico; the occurrence of multiple cold surges, which reinforce the anticyclone over Mexico; and the absence of low-latitude, upper-tropospheric, mobile short-wave troughs to prematurely weaken the anticyclone. Cold surges (especially COLD) can be associated with an acceleration of the trade winds over the eastern North Pacific Ocean and play a role in El Niño–Southern Oscillation. The results in this paper are compared to the results of previous studies of North American, Central American, and east Asian cold surges.

1. Introduction

Cold surges from the midlatitudes can have a substantial impact upon the weather and climate of the tropical atmosphere and ocean [see Schultz et al. (1997, sections 1 and 2) for a review]. A notable example was the cold surge into Mexico and Central America associated with the eastern United States Superstorm 1993 of 12–14 March (hereafter, SS93), described by Schultz et al. (1997). That surge brought surface winds gusting to 30 m s^{-1} and lower-tropospheric temperature decreases as large as 15°C into Mexico and Central America; the direct effects from that surge were felt as far equatorward as Panama [see Fig. 1 in Schultz et al. (1997) for a map showing geographical locations]. The cold surge also indirectly affected the tropical atmosphere and ocean as manifested by a 6°–8°C decrease in the sea surface temperature (SST) along the western coast of Mexico and Central America, a strengthening of the trade winds by about 5–10 m s^{-1} over the eastern North Pacific Ocean, and a possible enhancement of near-surface convergence and convection along the ITCZ (Schultz et al. 1997).

Another issue considered by Schultz et al. (1997) was why the SS93 cold surge reached such low latitudes (7°N) and was associated with such a large lower-tropospheric temperature decrease. They concluded that the dynamic forcing associated with the low-latitude upper-level trough and confluent jet-entrance region

* Current affiliation: NOAA/ERL/National Severe Storms Laboratory, Norman, Oklahoma.

Corresponding author address: David M. Schultz, NOAA/ERL/National Severe Storms Laboratory, 1313 Halley Circle, Norman, OK 73069.
E-mail: schultz@nssl.noaa.gov

over Mexico and Central America, in addition to topographic channeling along the Sierra Madre, favored the extraordinary equatorward incursion of the cold air. That case study, and the issues raised therein, suggests that a more comprehensive approach to examining cold-surge structure and evolution is required. As in Reding (1992) and Schultz et al. (1997), a Central American cold surge (CACS) is defined in this paper as the leading edge of a cold anticyclone originating poleward of Mexico that has penetrated equatorward to at least 20°N.

The principal goal of this research is to determine whether distinct categories of CACSs exist and, if so, to identify characteristic planetary- and synoptic-scale signatures associated with each category. This research differs from previous studies of North American cold-surge classification (e.g., Hill 1969; Dallavalle and Bosart 1975; Henry 1979; Rogers and Rohli 1991; Mecikalski and Tilley 1992) by presenting the signatures over a larger area, particularly equatorward of 15°N. The advantages of this enlarged study domain will be the ability to illustrate how the extratropical–tropical interactions differ for the various categories of CACSs and to facilitate qualitative comparison to the abundant literature on extratropical–tropical interaction associated with east Asian cold surges.

Section 2 presents some aspects of the climatology of cold surges and discusses Reding's (1992) database of events used for this study. Reding's climatology makes it possible to determine categories of CACSs based on their strength and longevity. In section 3, individual events from each category are averaged together to form composite events to illustrate the structure and evolution of the planetary- and synoptic-scale features, discriminating between the different categories of CACSs. The implications for El Niño–Southern Oscillation (ENSO) are discussed in section 4 and a brief summary is presented in section 5.

2. Climatology of Central American cold surges

A variety of studies employing different methodologies have shown that cold surges originating from the midlatitudes moving into Mexico and Central America are common occurrences during the cold season (e.g., Hill 1969; Klaus 1973; DiMego et al. 1976; Henry 1979; Reding 1992). Additionally, Hill (1969, 67–68) showed that 80%–95% of all negative changes in interdiurnal temperature in eastern Mexico during the cold season (November–April) were related to cold-frontal passages. We would therefore expect cold surges to occur often enough and with sufficient intensity to have an impact on the climatology of Mexico and Central America.

a. Regional radiosonde climatology

To test this hypothesis, a climatology is constructed from observational radiosonde data from seven different stations, all near 18°–21°N. These seven stations sample the east Pacific Ocean [Isla Socorro, Mexico (SOC)], eastern Mexico [Veracruz, Mexico (VER); Merida, Mexico (MID)], the Caribbean [Owen Roberts Airport, Grand Cayman (MWCR); Guantanamo Bay, Cuba (MUGM); San Juan, Puerto Rico (TJSJ)], and the Leeward Islands [Juliana Airport, St. Maarten (TNCM)]. The radiosonde data come from the National Center for Atmospheric Research–National Climatic Data Center (NCAR–NCDC) Radiosonde Data of North America, Version 1.0 compact disc for the years 1946–92 (Schwartz and Govett 1992). The mean and standard deviation of 1000-hPa temperature, 1000-hPa wind speed, and sea level pressure, and their mean values for each 10° increment in wind direction, for all available times during the cold season (November–April) for each station were calculated (Table 1).

Because these seven stations all lie along nearly the same latitude, variations in these parameters will indicate either longitudinally varying climatological features or local effects such as sea breezes. Table 1 shows that the three stations near a large body of land (VER, MID, and MUGM) have the lowest average 1000-hPa temperature ($\overline{T}_{1000}$),[1] largest standard deviation of 1000-hPa temperature ($\sigma_{T_{1000}}$), and lowest 1000-hPa temperature from a particular wind direction ($T_{\min}$), usually from the west through northeast directions. In particular, $T_{\min}$ at VER (19.6°C) is nearly one standard deviation (2.9°C) below the mean ($\overline{T}_{1000}$ = 22.2°C), illustrating the impact that northwest winds behind cold surges can have on the climate of VER. In addition, at VER and MID, the standard deviation of the sea level pressure ($\sigma_{p_{\mathrm{MSL}}}$) is higher than the other stations, since these stations are impacted by the periodic passage of anticyclones during the cold season, which tend to stay centered over (or near) landmasses. When the wind is from the north-northwest (330°–340°) at VER, the sea level pressure ($p_{\max}$) and the wind speed ($V_{\max}$) are both a maximum, about a standard deviation greater than their mean values, indicating the extent to which cold surges impact the local climatology. Progressing farther east (MWCR, MUGM, TJSJ, TNCM), the wind direction associated with $T_{\min}$ turns from the northwest to the northeast, as the northeast trade winds are reinforced by cold anticyclones passing off North America and moving eastward poleward of these stations. Also, under the influence of a more maritime tropical climate, the variability in sea level pressure and wind speed decreases (Table 1).

These results from Table 1 indicate that lower temperatures, stronger wind speeds, and higher pressures accompany the lower-tropospheric north-northwesterly winds associated with cold surges. These cold surges affect the climate of eastern Mexico (e.g., VER and

[1] The low $\overline{T}_{1000}$ at SOC occurs because of the climatologically cool water off the west coast of North America.

TABLE 1. Climatology of radiosonde data for seven stations lying along 18°–21°N. Lat (Long) is the latitude (longitude) of the station. Here, ''Elev.'' is the station elevation, N_{1000} is the number of observations composing the climatology, $N_{<1000}$ is the number of observations with $p_{msl} < 1000$ hPa excluded from the climatology, $\overline{T}_{1000}$ is the average 1000-hPa temperature for all wind directions, $\sigma_{T_{1000}}$ is the standard deviation of the 1000-hPa temperature for all wind directions, and T_{min} is the minimum average 1000-hPa temperature among each 10° increment of wind direction and occurs from the direction $\phi_{T_{min}}$ (e.g., 340° represents an average of all events when the wind direction is 340°–349°). ''Range'' represents a subjective determination of the wind directions accompanying temperatures below the mean (wind directions must comprise at least 1% of the total number of observations). Here, $\overline{p}_{MSL}$ is the average sea level pressure, $\sigma_{p_{MSL}}$ is the standard deviation of the sea level pressure, p_{max} is the maximum average sea level pressure among each 10° increment of wind direction and occurs from the direction $\phi_{p_{max}}$, $\overline{V}_{1000}$ is the average 1000-hPa wind speed, $\sigma_{V_{1000}}$ is the standard deviation of the 1000-hPa wind speed, and V_{max} is the maximum average 1000-hPa wind speed among each 10° increment of wind direction and occurs from the direction $\phi_{V_{max}}$.

Stat. name		Isla Socorro	Veracruz	Merida	Grand Cayman	Guantanamo Bay	San Juan	St. Maarten
Stat. no.		SOC 76723	VER 76692	MID 76644	MWCR 78384	MUGM 78367	TJSJ 78526	TNCM 78866
Lat	(°N)	18.72	19.12	20.98	19.28	19.89	18.43	18.05
Long	(°W)	110.95	96.12	89.65	81.34	75.15	66.00	63.12
Elev.	(m)	35	35	9	3	17	19	9
N_{1000}		2298	7070	11 365	12 476	7733	15 884	7173
$N_{<1000}$		0	6	5	0	5	3	1
$\overline{T}_{1000}$	(°C)	21.9	22.2	23.6	24.5	23.2	23.7	24.4
$\sigma_{T_{1000}}$	(°C)	1.7	2.9	3.7	1.2	2.3	1.1	1.0
T_{min}	(°C)	20.9	19.6	21.8	22.8	21.6	23.4	23.7
$\phi_{T_{min}}$	(°)	340	320	070	010	350	120 & 130	020
Range	(°)	300–010	260–340	320–100	360–050	330–060	020–150	020–080
$\overline{p}_{MSL}$	(hPa)	1011.5	1012.7	1013.6	1014.2	1012.6	1015.1	1015.4
$\sigma_{p_{MSL}}$	(hPa)	3.2	5.2	4.0	1.8	2.4	1.8	1.7
p_{max}	(hPa)	1012.9	1017.1	1015.8	1015.5	1013.8	1016.0	1016.0
$\phi_{p_{max}}$	(°)	030	330	060	020	050	080	070
$\overline{V}_{1000}$	(m s^{-1})	3.7	5.6	5.6	5.7	3.9	5.5	6.6
$\sigma_{V_{1000}}$	(m s^{-1})	1.8	3.0	1.8	2.2	1.7	2.2	2.1
V_{max}	(m s^{-1})	5.2	9.4	6.2	7.0	5.1	7.1	7.2
$\phi_{V_{max}}$	(°)	040	340	040	050	100	070	070

MID) to a greater degree compared to other stations at the same latitude. Furthermore, it would be useful to know the variability of characteristics of individual cold surge events for comparison with other events in the past and the climatology in Table 1. For example, if the SS93 cold surge was unusually strong compared to other events (as measured by, e.g., the temperature decrease behind the surge and the latitude of most equatorward extent), then understanding the conditions that are favorable for strong surges could lead to improved forecasting of such events. [The difficulty that numerical weather prediction models have predicting cold surges has been noted by Colucci and Bosart (1979), Grumm and Gyakum (1986), Weiss (1992), and Mesinger (1996).]

b. Reding's methodology

Reding (1992) compiled a table of CACS events that occurred during the 11 cold seasons (October–March) from 1979–80 through 1989–90. Reding identified cold fronts over the southern United States using the National Centers for Environmental Prediction (previously known as the National Meteorological Center) Northern Hemisphere surface analyses and tracked them into Central America using hourly satellite imagery. He then reviewed the hourly surface observations from MID for each potential cold surge and found good agreement between the surface frontal passage as determined from the satellite imagery and a daily maximum temperature decrease of 4°C or more at MID within 48 h after frontal passage and sustained surface winds from 300° to 030° for more than 24 h after frontal passage. For the 11-cold-season period, Reding (1992, 166–176) identified 177 CACS events—an average of 16.1 per cold season. This value is consistent with results from other climatologies, despite a variety of criteria and methodologies (Schultz et al. 1997, section 2b).

For each event, Reding recorded the onset date at MID, duration D, maximum equatorward penetration (or minimum latitude, ϕ_{min}), and the largest decrease in the daily maximum temperature at MID within 48 h after frontal passage (ΔT). He defined the duration of the event as ''the time, in days, between CACS onset at MID and when cloud features [evident on the satellite imagery] indicate east-northeast low-level trade wind flow has regained control over all of Central America'' (Reding 1992, 33). The maximum equatorward penetration was defined as ''the southernmost location at which cloud features indicate northerly–northwesterly low-level cold surge flow is affecting the Central American land mass'' (Reding 1992, 33).

As an independent test of Reding's data, we examined

the radiosonde data for CACS events using his criteria (modified slightly to account for the different temporal resolution of the sounding data versus the surface/satellite data used by Reding: 12 h versus 1 h). The radiosonde data for all available times during the cold season (October–March) at MID from 1957 to 1989 were searched for all events in which the 0000 UTC surface temperature on consecutive days decreased by 4°C or more (ΔT_r) and the surface winds were from 300° to 030° (including calm) for at least 24 h. The duration of the event was then defined as the number of days during which the winds remained between 300° and 030°.

Of the 363 cases identified from the MID radiosonde data by our criteria (averaging 11.0 events per cold season), 97 occurred during the same period as Reding's 177 events. Of these 97, 70 (72%) were also included in Reding's dataset. For the 80 events that were identified by Reding's criteria but not ours, the primary reasons why they were not selected were (a) small ΔT (4°–6°C) and smaller ΔT_r. (<4°C) (likely due to the maximum temperature the day before onset being reached before 0000 UTC), (b) missing radiosonde data, or (c) cold-surge events that did not meet the wind criterion. Of the 27 events (28%) that were not part of Reding's cases, most had a small ΔT_r of 4°–6°C or were associated with anticyclones that either rapidly dissipated over the Gulf of Mexico or passed over the southeast United States, only obliquely affecting MID. An inspection of daily horizontal (e.g., surface, 850, 500 hPa) maps for many of these CACSs indicate that their structure and evolution were similar to those selected by Reding. Therefore, despite the differences in the way the duration and temperature change were calculated at MID, our results for a longer time period are comparable to Reding's (1992). This comparison provides additional support for the usefulness of Reding's listing of CACS events and gives us confidence to proceed with our analysis based upon his data.

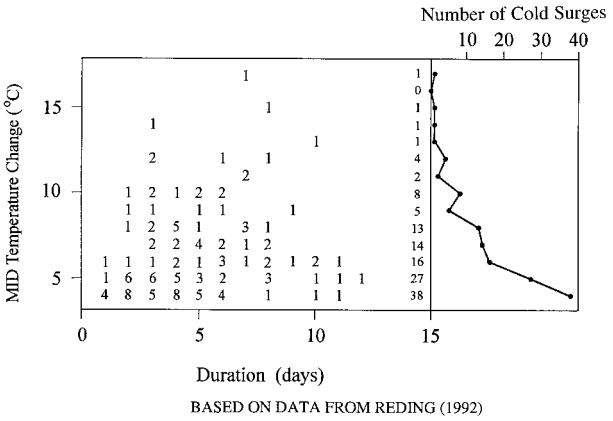

FIG. 1. Frequency of duration (D, in days) vs daily maximum temperature change at MID within 48 h after frontal passage [ΔT (°C), defined in the text]. Plotted numbers represent the number of events in the 11-cold-season period used by Reding (1992). The right-hand side presents a line graph of the number of events as a function of the daily maximum temperature change at MID within 48 h after frontal passage. Plotted values for frequencies may not add up to the totals on the vertical axis of the line graph since some events may be missing duration values.

c. Frequency plots

A frequency plot based on Reding's data of the number of cold surges as a function of temperature change at MID and duration is shown in Fig. 1. On the right-hand side of Fig. 1 is a line graph of the number of cold surges over Reding's 11-cold-season period as a function of ΔT showing that the number of CACSs decreases as ΔT increases from 4°C [the minimum criterion for a CACS defined by Reding (1992)] to a maximum of 17°C. On the left side of Fig. 1, the number of cold surges as a function of both ΔT and D is displayed. Both short- (1 day) and long- (11–12 days) duration events are characterized by relatively small temperature changes, which may be due to the small sample size for these extreme values. Otherwise, there is no obvious relationship between ΔT and intermediate values of D (2–10 days), suggesting that large temperature decreases behind the cold surge are not necessarily associated with more persistent events. Apparently the process or processes that affect the longevity of CACSs show little sensitivity to the temperature decrease associated with the surge (a point made again in section 3e).

In Fig. 2 the relationship between the duration of cold surges and their maximum equatorward extent is examined. Along the top of Fig. 2 is a line graph of the number of cold-surge events during the 11-cold-season period as a function of D, showing that 75% of the cold surges tend to persist for 2–6 days with a maximum at 3–4 days; the curve decreases sharply at one day, and is skewed toward longer durations, reaching a maximum of 13 days. We believe that it is no coincidence that the typical duration of cold surges (2–6 days) is approximately the same timescale as the period between mobile disturbances in the westerlies and their associated surface cyclogenesis (e.g., Bjerknes and Solberg 1922, 17–18; Hill 1969, 6; Blackmon 1976). These results are consistent with Colle and Mass (1995, their Fig. 27e) and Schultz et al. (1997, their Figs. 9b,d), who show that the cessation of the northerlies over northern Mexico (the source of cold, high-momentum air for the surge farther equatorward) was attributed to the approach of an upper-level short-wave trough, resulting in pressure falls over eastern Mexico and increasing southerlies, several days after the initiation of the cold surge.

The bottom of Fig. 2 indicates a trend (roughly marked by the dashed line) for surges that penetrate to low latitudes to persist longer than those that do not penetrate to low latitudes, in agreement with Henry (1979, his Table 3). The spread for any given value of D or $\phi_{\min}$, however, can be rather substantial, resulting

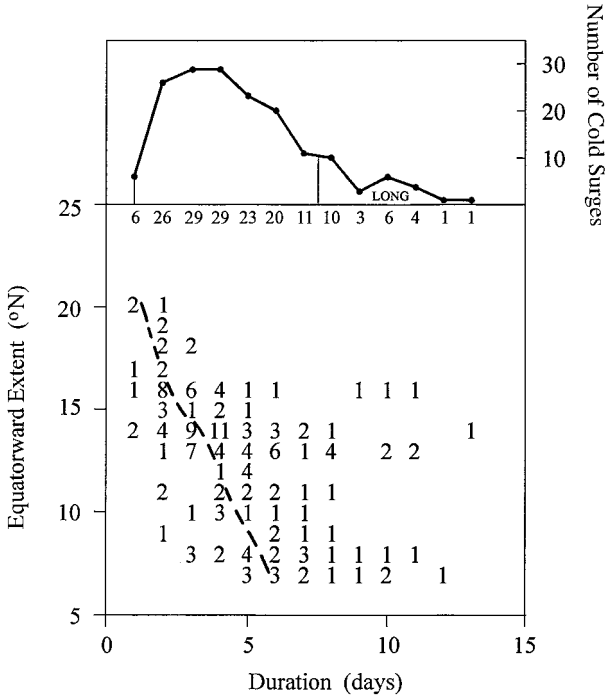

FIG. 2. Frequency of duration (D, in days) vs most equatorward extent [ϕ_{min} (°N), defined in the text]. Plotted numbers represent the number of events in the 11-cold-season period used by Reding (1992). The dashed line represents the approximate axis of maximum frequency. The top presents a line graph of the number of events as a function of duration. Plotted values for frequencies may not add up to the totals on the axis of the line graph since some events may be missing most-equatorward-extent values. The label LONG represents cases selected for the LONG composite.

in limited value as a predictive tool. There is, however, an absence of medium- and long-lived surges (four days or greater) when $\phi_{min} \geq 17°$N, indicating that surges that do not reach Honduras are more susceptible to cessation by ensuing mobile short-wave troughs in the upper-level westerlies.

A reasonable hypothesis might be that relatively low-latitude surges would be less likely to occur since the terminus of the cold surge in Central America lies so far equatorward from the source region of the cold air. Inspection of Fig. 2 indicates that this hypothesis does not appear to be valid. Indeed, Fig. 3 addresses this apparent contradiction as its right-hand side illustrates the number of CACSs during the 11-cold-season period as a function of the latitude of most equatorward extent. There are four main latitude bands where CACSs tend to reach their most equatorward extent: 16°, 13°–14°, 11°, and 7°–8°N. Three of these regions appear to be due to topographical barriers that impede the advance of the cold surge [see Schultz et al. (1997, Fig. 1) for topography]: the abrupt right-angle bend of the Sierra Madres in Honduras at 16°N, the ridge of mountains in Costa Rica equatorward of Lake Nicaragua at 11°N, and the Panamanian isthmus and mountains of northern Colombia at 7°–8°N (Reding 1992, 41). The fourth, and largest, maximum in Fig. 3 at 13°–14°N lies along a relatively flat topographic area on the Atlantic coast of Nicaragua, appearing to rule out orographic effects; presently, we have no satisfactory explanation for this maximum.[2]

The left-hand side of Fig. 3 illustrates the relationship between ΔT and ϕ_{min}. While there is a tendency for the coldest surges (those with the largest ΔT) to penetrate deepest into the Tropics (those labeled COLD), this is certainly not the rule. In fact, some surges with small ΔT (4°–5°C) also reach as far equatorward as 7°N (those labeled COOL), whereas many cold surges with ΔT greater than or equal to 8°C stall at relatively high latitudes (13°–18°N). This would appear to be at odds with a hypothesis that those CACSs bearing the largest temperature difference would travel the farthest equatorward, akin to gravity currents (e.g., Simpson 1987, 40). Also apparent from Fig. 3 is that the CACS associated with SS93 (its location, were it to be included among this data, is circled and labeled SS'93) would be tied for the second most intense cold surge.

3. Composite analyses of Central American cold surges

To identify the planetary- and synoptic-scale features associated with CACSs possessing different characteristics (e.g., low-latitude, long-duration), groups of cases are selected from Reding's dataset from which composites can be constructed to illustrate average cold-surge life cycles.

a. Methodology

The European Centre for Medium-Range Weather Forecasts (ECMWF) 2.5° latitude × 2.5° longitude initialized analyses from December 1978 through December 1989 (December 1979 missing) on isobaric surfaces are used to create the composite fields from the individual CACS events. As noted by Bengtsson et al. (1982, 33–34), ECMWF calculates geopotential height

[2] One hypothesis for the occurrence of this maximum might be that surges are slowed as they reach the northern extent of the strong climatological easterlies north of South America around this latitude (Hastenrath 1967) and perhaps merge with them (Schultz et al. 1997). Another hypothesis is that there may be enough leakage of cold air through the gap in the Central American mountains near Lake Nicaragua to limit the further equatorward progression of fronts at this latitude or that the cold air associated with some surges, having advanced equatorward of the Honduran mountains, becomes too shallow to progress farther and is quickly modified by sensible heating. A third possible explanation may lie in Reding's satellite-image interpretation criteria for ϕ_{min}. It may be possible that there is a climatological limit to the trade-wind stratocumulus that may be affecting the interpretation of his results.

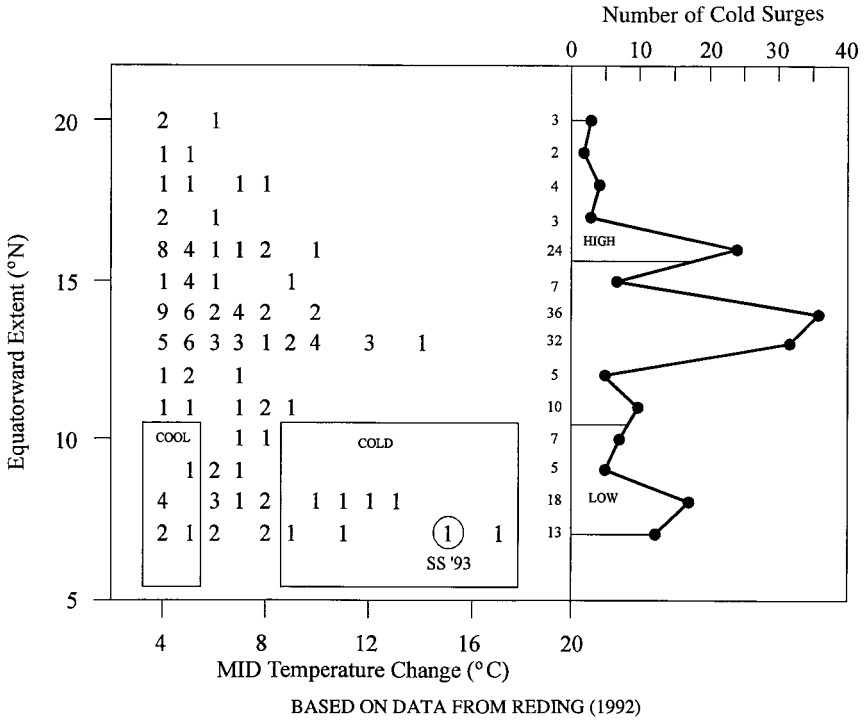

FIG. 3. Frequency of daily maximum temperature change at MID within 48 h after frontal passage [ΔT (°C)] vs most equatorward extent [ϕ_{min} (°N), defined in the text]. Numbers represent the number of events in the 11-cold-season period used by Reding (1992). A circle and the notation SS'93 represent the location of the CACS associated with Superstorm 1993 (13 March) (Schultz et al. 1997), if it were included in this dataset; note that it is coincident with an event from Reding (1992). The labels HIGH, LOW, COLD, and COOL represent cases selected for those individual composites. (LOW composites not shown in this paper.) The right-hand side presents a line graph of the number of events as a function of the latitude of most equatorward extent. Plotted values for frequencies may not add up to the totals on the axis of the line graph since some events may be missing daily maximum temperature change values.

fields for pressure levels below ground by extrapolating from the observed mean sea level pressure deviations and the model first-guess temperatures. Although weather features over Mexico, Central America, and the North Atlantic and North Pacific Ocean basins investigated in this study are not found in regions of abundant data, we believe the analyses are adequate for the present study. As discussed by Trenberth and Olson (1988) and Trenberth (1992, 1, 4), the ECMWF analyses are believed to be the best available for general research. The quality of the analyses in the midlatitudes is high (Trenberth and Olson 1988) and the analyses have been employed in numerous studies. Even in the Tropics, the ECMWF analyses have been useful for a variety of planetary- and synoptic-scale studies [e.g., see Molinari et al. (1997)]. More specific discussion of the ECMWF analyses and their shortcomings is found in Hoskins et al. (1983, 1610–1611) and Trenberth (1992).

To examine the composite CACSs that reach high latitudes (large ϕ_{min}), all CACSs based on Reding's list of events for which ECMWF analyses are available are selected where ϕ_{min} is greater than or equal to 16°N (see right side of Fig. 3). This criteria selects 33 cases, which are then averaged together at 1200 UTC (to minimize diurnal effects) on the onset date of each surge (hereafter day 0) to produce the composite high-latitude cold-surge event (hereafter HIGH). Time-lagged composites are then created. For example, day −3 indicates the composite of all events three days (72 h) prior to 1200 UTC on the onset date of each individual event.

While most of the events comprising HIGH possess relatively modest ΔT, cases where ϕ_{min} is less than or equal to 10°N (LOW in Fig. 3) possess a large range of ΔT (COLD versus COOL in Fig. 3). Two composites of eight cases each are therefore constructed: COLD ($\Delta T \geq 9$°C) and COOL (4°C $\leq \Delta T \leq$ 5°C). The individual CACS events upon which the COLD and COOL composites are based are listed in Tables 2 and 3, respectively.

To investigate the longevity of cold surges (i.e., why some surges persist for as long as 13 days while others persist only for a few days; see, e.g., Fig. 2), one final pair of composites is created based on the duration of the surge D. To create the long-duration composite cold surge (LONG), 24 CACS events (Table 4) are selected that persist for $D \geq 8$ days (top of Fig. 2). Another

TABLE 2. Cases that the COLD composite comprises: Cold-surge events that reach low latitudes ($\phi_{min} < 10°N$) with a large daily maximum temperature change at MID within 48 h after frontal passage ($\Delta T \geq 9°C$). Parameters defined in section 2b. Data from Reding (1992).

Onset date	$\overline{\phi}_{min}$ (°N)	ΔT (°C)	D (days)	Prior surge (days)
6 Mar 1989	7	17	7	12
22 Dec 1989	7	15	8	9
22 Feb 1989	7	11	7	13
6 Feb 1987	7	9	9	12
21 Mar 1986	8	13	10	20
2 Mar 1980	8	12	3	5
3 Jan 1985	8	11	7	27
1 Feb 1980	8	10	5	8
Average	7.5	12.3	7.0	13.3
Std dev	0.5	2.5	2.1	6.6

TABLE 3. Cases that the COOL composite comprises: Cold-surge events that reach low latitudes ($\phi_{min} < 10°N$) with a small daily maximum temperature change at MID within 48 h after frontal passage ($\Delta T = 4°–5°C$). Parameters defined in section 2b. Data from Reding (1992).

Onset date	$\overline{\phi}_{min}$ (°N)	ΔT (°C)	D (days)	Prior surge (days)
16 Jan 1981	7	4	5	5
3 Dec 1981	7	4	10	12
29 Dec 1983	7	5	12	4
17 Dec 1980	8	4	6	5
18 Dec 1981	8	4	5	3
6 Nov 1984	8	4	3	37
28 Oct 1987	8	4	6	27
15 Feb 1985	9	5	2	4
Average	7.8	4.3	6.4	12.1
Std dev	0.7	0.4	3.2	12.0

composite is generated at 1200 UTC on the date of cessation (the onset date plus the duration) at which each individual long-duration surge ends. This composite is hereafter referred to as LONGC.

Anomaly fields are defined as departures of the composite fields from weighted monthly climatological values; that is, the climatological field is constructed from monthly averages that are weighted according to the number of events with onset dates in each month. For example, the climatological fields for the COLD composite (Table 2) are constructed by multiplying the December, January, February, and March climatological fields by 1/8, 1/8, 3/8, and 3/8, respectively, and summing the results. Likewise, differently weighted climatologies are created for the other composites (e.g., the weights for COOL and LONG are obtained from the number of events in each month in Tables 3 and 4, respectively). The monthly mean climatological fields are the ECMWF analyses for the 10-yr period 1979–88. The two-tailed Student's t-test is used to express the probability that the composite (mean) is statistically different from climatology (Panofsky and Brier 1968). Unless noted otherwise, the anomalies discussed in this paper are statistically significant to at least the 95% confidence level, with most anomalies significant to 99% (not shown).

We begin by examining the differences in the planetary- and synoptic-scale patterns between CACSs, which penetrate far equatorward but have large and small ΔT (COLD and COOL, respectively).

b. COLD

To illustrate the upper-level nondivergent flow, the COLD 200-hPa streamfunction composite and anomaly fields from the weighted climatology at days -3, -1, $+1$, and $+3$ are presented in Fig. 4. Three days prior to the onset of the cold surge at MID, the planetary-scale flow consisted of a stronger-than-normal jet stream over the eastern United States and the western North Atlantic Ocean (as indicated by the low streamfunction anomaly poleward of the jet and the high anomalies within and equatorward of the jet) (Fig. 4a). The jet stream over the central North Pacific Ocean, on the other hand, was weaker than normal and shifted slightly equatorward (as indicated by the high streamfunction anomaly west of Alaska poleward of the low anomaly centered near 30°N, 170°W), and the jet-exit region over the eastern North Pacific was anomalously diffluent (as indicated by the high streamfunction anomaly poleward of the low streamfunction anomaly at 10°N, 135°W). By day -1, an amplifying trough in the jet at 145°W

TABLE 4. Cases that the LONG composite comprises: Cold-surge events that have a long duration ($D \geq 8$ days). Here, M is missing data and the asterisk is the first event of the cold season. Parameters defined in section 2b. Data from Reding (1992).

Onset date	ϕ_{min} (°N)	ΔT (°C)	D (days)	Prior surge (days)
1 Oct 1987	14	M	13	*
29 Dec 1983	7	5	12	4
28 Nov 1988	13	5	11	6
11 Jan 1983	8	6	11	9
20 Jan 1983	13	4	11	3
8 Oct 1988	16	M	11	*
1 Oct 1983	16	M	10	*
21 Jan 1989	13	6	10	36
9 Jan 1986	7	6	10	15
3 Dec 1981	7	4	10	12
1 Mar 1987	13	5	10	13
21 Mar 1986	8	13	10	20
25 Jan 1988	8	M	9	4
6 Feb 1987	7	9	9	12
3 Oct 1980	16	6	9	*
4 Nov 1982	11	5	8	19
2 Jan 1983	14	7	8	17
19 Oct 1989	13	8	8	*
17 Dec 1980	8	4	8	5
4 Feb 1984	13	7	8	8
22 Dec 1989	7	15	8	9
30 Nov 1987	9	6	8	10
30 Nov 1989	13	5	8	6
28 Nov 1979	13	6	8	16
Average	11.1	6.6	9.5	11.8
Std dev	3.2	2.8	1.4	7.6

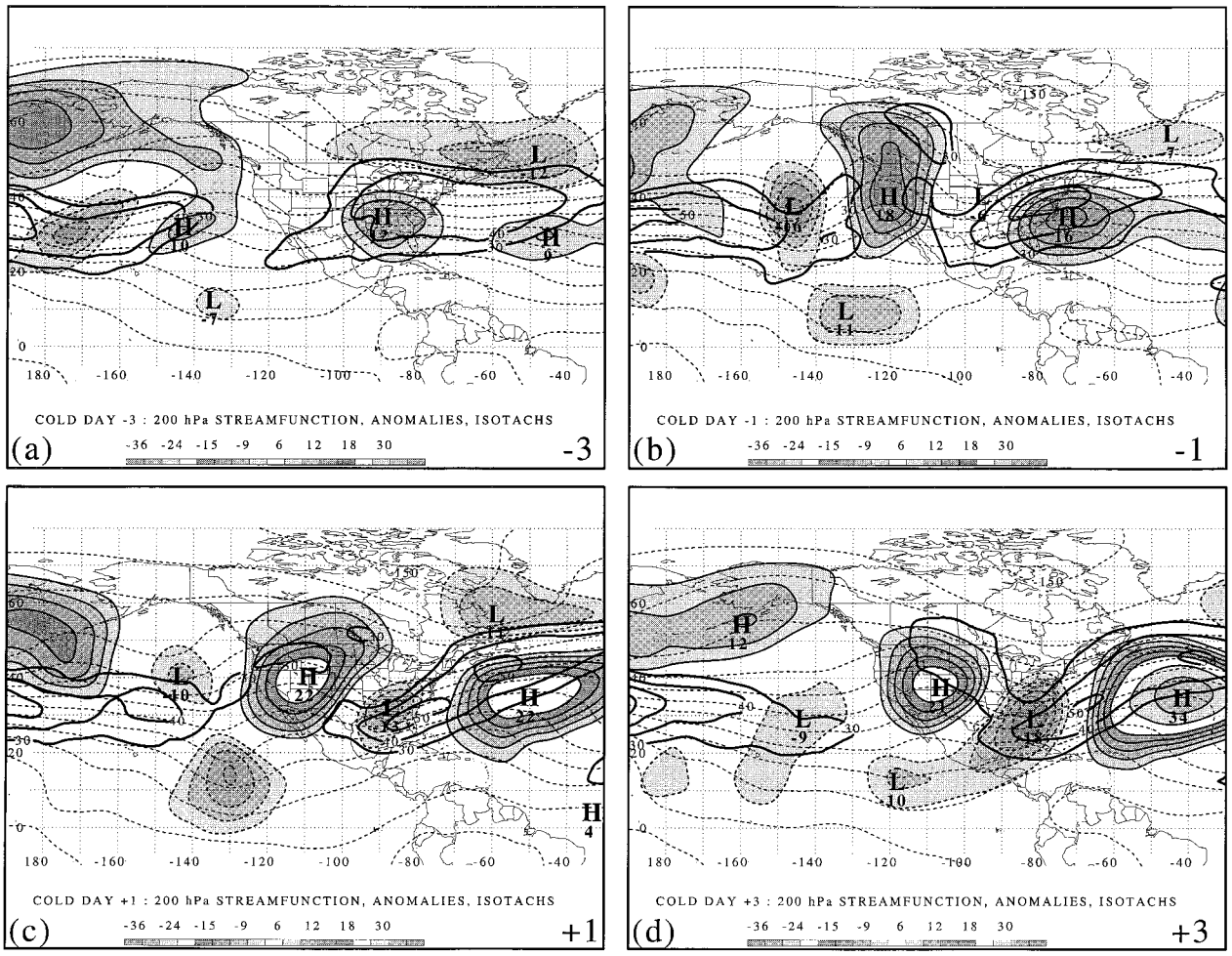

FIG. 4. COLD: 200-hPa composite streamfunction (thin dashed lines every 15×10^{-6} m^2 s^{-1}), streamfunction anomalies from weighted climatology [$\times 10^{-6}$ m^2 s^{-1}, contoured and shaded according to scale at bottom of figure; solid (dashed) lines surround positive (negative) values], and 200-hPa composite isotachs of total horizontal wind (thick solid lines every 10 m s^{-1} starting at 30 m s^{-1}): (a) day -3, (b) day -1, (c) day $+1$, (d) day $+3$.

was associated with strong ridge-building over the Pacific coast of North America and a deepening trough at 10°N, 130°W (Fig. 4b), reminiscent of the positive phase of the Pacific–North American pattern (Wallace and Gutzler 1981, their Fig. 17a). This low-latitude trough suggests a stronger-than-normal westerly duct near the equator favoring cross-equatorial communication (Webster and Holton 1982) and, in association with the ridge off the east coast of the United States, resulted in southwesterly flow over Mexico into a strong, low-latitude, subtropical jet-entrance region over the Gulf of Mexico by day $+1$ (Fig. 4c). This confluent jet-entrance region is consistent with that for the SS93 cold surge (Schultz et al. 1997, their Figs. 5c and 6d), in which the direct secondary circulation associated with the upper-level jet-entrance region (e.g., Beebe and Bates 1955; Uccellini and Johnson 1979) favored subsidence across northern Mexico and the southern United States with low-level northerlies farther equatorward (Schultz et al. 1997, their Figs. 7 and 8). The subsidence on the poleward side of the jet-entrance region (acting in concert with the upstream ridge) maintains the anticyclone at low latitudes and the low-level northerlies [acting in concert with the topographically forced northerlies (Colle and Mass 1995)] maintains the equatorward movement of the anticyclone. A similar interaction between cold surges and jet stream circulations has been discussed in east Asia (e.g., Chang and Lau 1980; Lau et al. 1983; Chu and Park 1984; Boyle 1986b; Lau and Chang 1987). By day $+3$ (Fig. 4d), the eastern United States trough continued to deepen while moving eastward across Florida as the ridge downstream over the Atlantic amplified in a manner reminiscent of downstream development (e.g., Joung and Hitchman 1982; Lau et al. 1983; Orlanski and Sheldon 1995).

The corresponding 1000-hPa geopotential height (hereafter height) composite and anomaly fields are presented in Fig. 5 to illustrate the structure and evolution

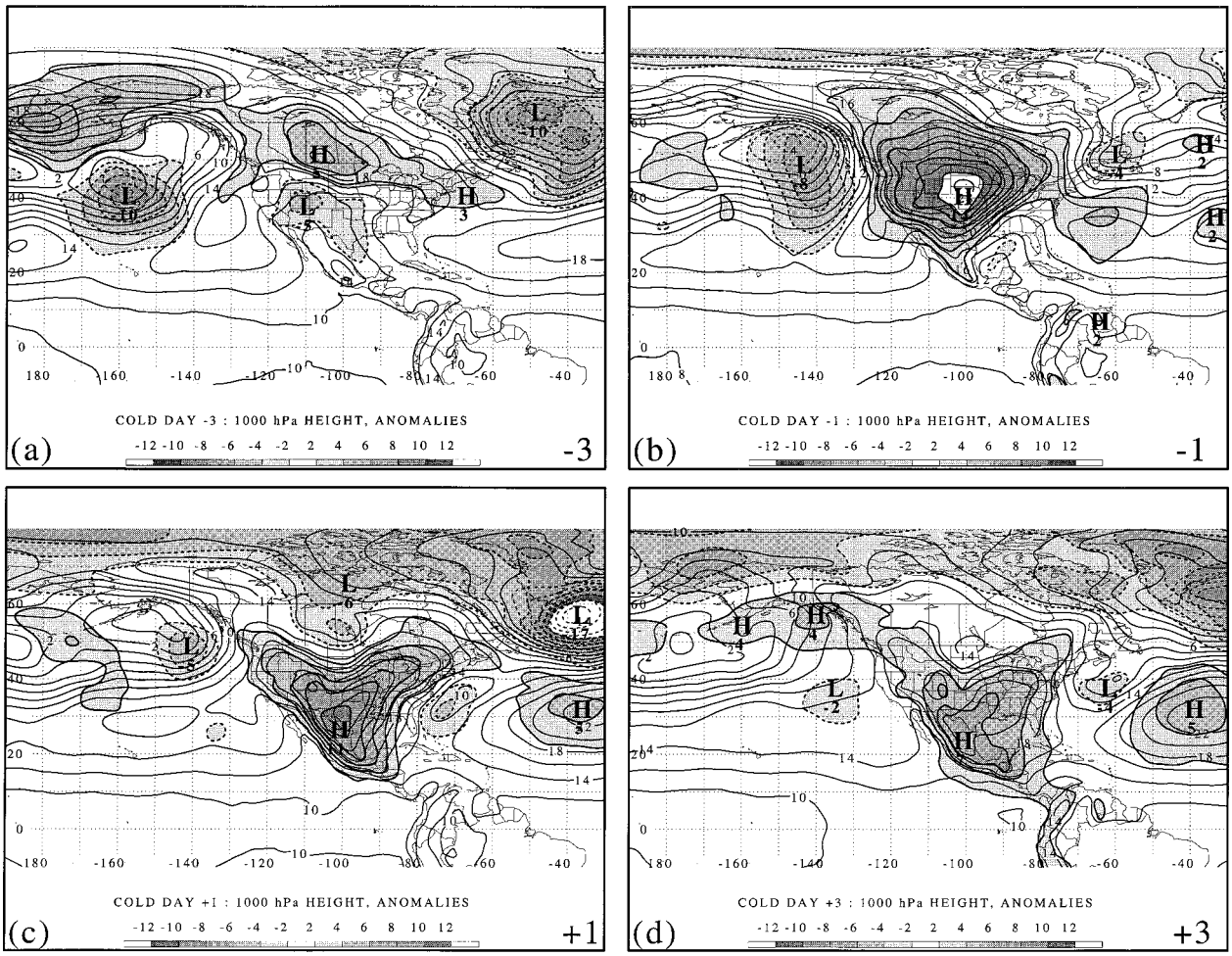

FIG. 5. COLD: 1000-hPa composite geopotential height (solid lines every 2 dam), and geopotential height anomalies from weighted climatology [dam, contoured and shaded according to scale at bottom of figure; solid (dashed) lines surround positive (negative) values]: (a) day −3, (b) day −1, (c) day +1, (d) day +3.

of the lower-tropospheric features. The arrival of a cyclone into the Gulf of Alaska (Figs. 5a,b) associated with the upper-level short-wave trough exiting the North Pacific jet and strong ridge-building over the western United States (Figs. 4a,b) resulted in downstream trough formation over the central United States, leading to the initiation of the equatorward movement of the anticyclone associated with the cold surge. As noted by Dallavalle and Bosart (1975), Boyle and Bosart (1983), Konrad and Colucci (1989), Mecikalski and Tilley (1992), Colle and Mass (1995), and Schultz et al. (1997), among others, the equatorward movement of the anticyclone is accompanied by the departure of a short-wave trough from the western United States upper-level ridge. Additionally, this evolution is consistent with that of east Asian cold surges in which an intensifying upper-level short-wave trough downstream of a high-amplitude Siberian ridge initiates the cold surge (e.g., Chang and Lau 1980, 1982; Joung and Hitchman 1982; Lau and Lau 1984; Boyle 1986a; Boyle and Chen 1987; Wu and Chan 1997). The anticyclone in COLD originated over Alaska and south-central Canada, strengthened, expanded, and advanced equatorward by day −1 (Figs. 5a,b). [The above-normal height in Alaska prior to cold-surge onset east of the Rocky Mountains has been recognized as early as Henry et al. (1916, 345).] The great expanse of anomalously high height over the central United States was notable for the absence of any southwesterly flow across the Rockies, which would favor downslope warming and lower the 1000-hPa height (Fig. 5a). The anticyclone migrated farther equatorward along the Sierra Madre so that, by day +1, the anticyclonic height anomaly was centered over northern Mexico (Fig. 5c). By day +3, the composite 1000-hPa anticyclone was being pulled apart in two directions: one headed equatorward along the Sierra Madre and another moving eastward over the Ohio River valley (Fig. 5d), suggesting that both orography/sensible heating (Colle and Mass 1995) and dynamical processes, respectively, were affecting the movement of the

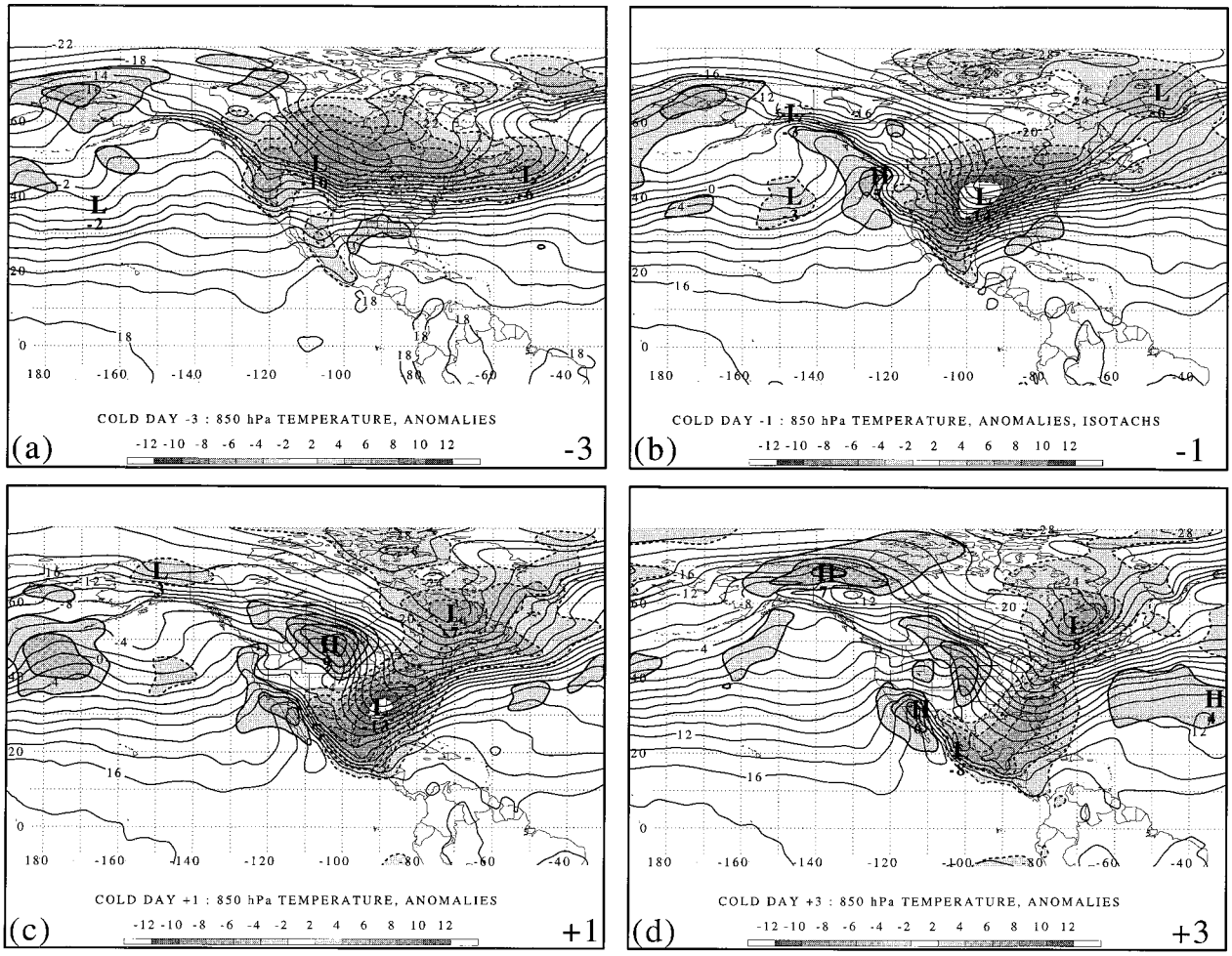

FIG. 6. COLD: 850-hPa composite temperature (solid lines every 2°C), and temperature anomalies from weighted climatology [°C, contoured and shaded according to scale at bottom of figure; solid (dashed) lines surround positive (negative) values]: (a) day −3, (b) day −1, (c) day +1, (d) day +3.

anticyclone [see also Mecikalski and Tilley (1992, Fig. 5c); Colle and Mass (1995, Fig. 3); Schultz et al. (1997, Fig. 16)]. Along with a strengthening anticyclone at 40°W (Figs. 5b–d), the col between the two highs formed a hyperbolic deformation zone (e.g., Bergeron 1928) along 70°W, which would favor frontogenesis and maintain stalling fronts in this region. During days −3 to +1, a weak 1000-hPa cyclone, associated with the 200-hPa trough over the southeast United States (Fig. 4c), moved from over the southwest United States, redeveloped over the Gulf of Mexico, and traveled poleward along the East Coast (Figs. 5a–d), similar to the ''cold southeast United States'' composite of Dickson and Namias (1976).

To demonstrate the magnitude and areal extent of the lower-tropospheric cooling associated with the cold surge, the 850-hPa temperature composite and anomaly fields are shown in Fig. 6. Three days before the surge onset (Fig. 6a), anomalously low temperatures associated with the 1000-hPa anticyclone (Fig. 5a) dominated much of the northern United States and southern Canada while anomalously high temperatures (~2°C) were found along the Gulf Coast of the United States. During days −1 through +1, the cold air expanded and was channeled equatorward along the mountains (Figs. 6b,c). By day +3, cooling on the order of 2°–4°C had spread all the way into northwestern Colombia, maximized along the Sierra Madre, across the Gulf of Mexico, and along the east coast of the United States on the east side of the 1000-hPa anticyclone (Figs. 5d, 6d). The 200-hPa ridge-building over the Pacific coast (Figs. 4a–c) was associated with warming in the lee of the northern Rockies (Figs. 6c,d), which induced the trough in the surface anticyclone in this region (Figs. 5c,d).

The 850-hPa streamfunction composite and anomaly fields and composite isotachs are shown in Fig. 7 to illustrate the evolution of the lower-tropospheric nondivergent wind field, particularly in the Tropics where height gradients are weak. The amplifying trough over the eastern North Pacific Ocean and ridge over the west-

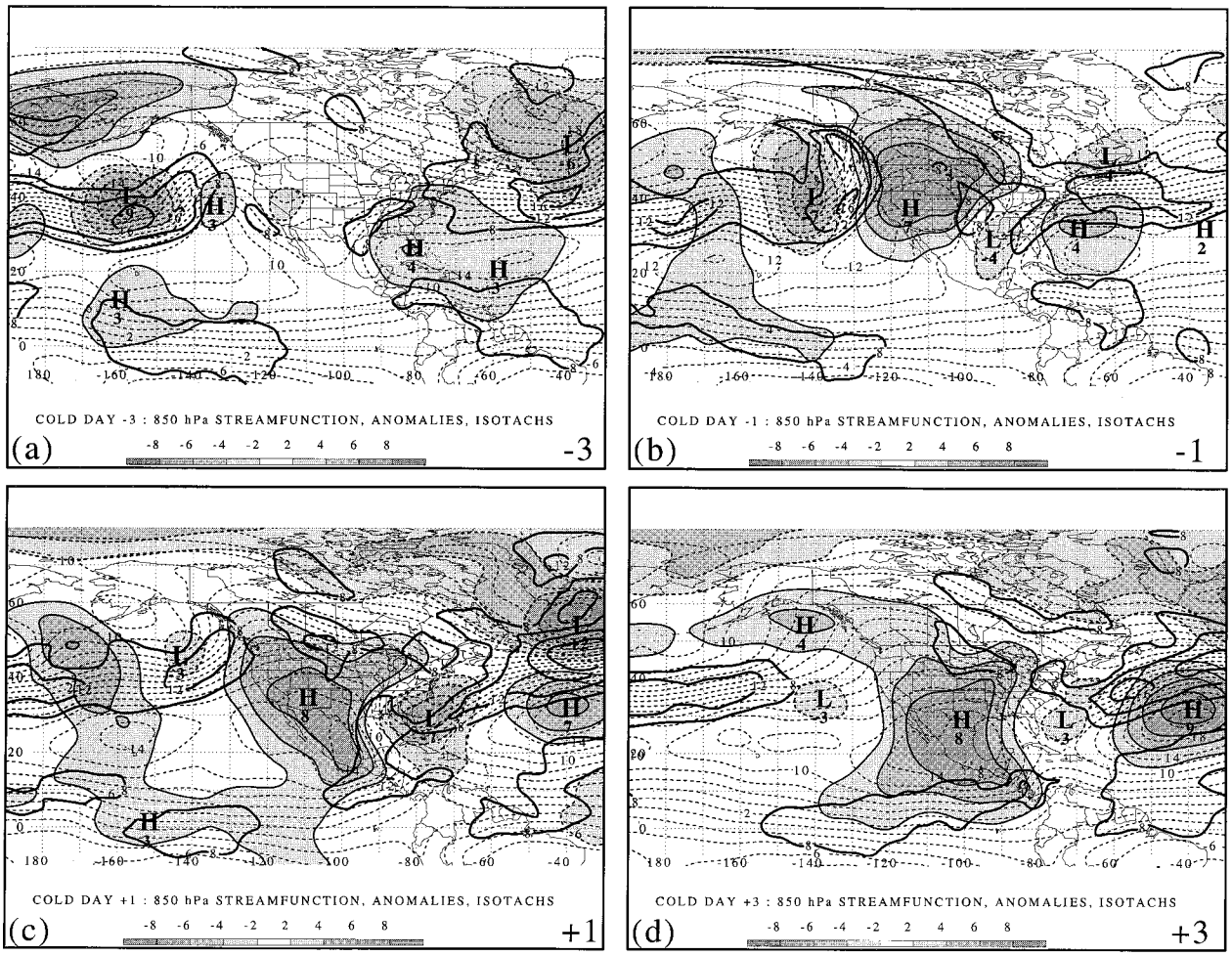

FIG. 7. COLD: 850-hPa composite streamfunction (thin dashed lines every 2×10^{-6} m^2 s^{-1}), streamfunction anomalies from climatology [$\times 10^{-6}$ m^2 s^{-1}, contoured and shaded according to scale at bottom of figure; solid (dashed) lines surround positive (negative) values], and 850-hPa composite isotachs of total horizontal wind (thick solid lines every 4 m s^{-1} starting at 8 m s^{-1}): (a) day -3, (b) day -1, (c) day $+1$, (d) day $+3$.

ern United States were apparent from days -3 to -1, as was an anticyclonic anomaly over the Caribbean with strong easterly trade winds on its equatorward flank near Nicaragua (Figs. 7a,b). The arrival of the cold surge and its associated anticyclonic circulation into Mexico resulted in strong northerly flow in the Gulf of Tehuantepec and northeasterly flow in the Gulf of Papagayo, whereas the developing col over the Caribbean caused the wind maximum north of South America to weaken (Fig. 7c). By day $+3$ (Fig. 7d), the flow across Central America was composed of the confluence of two air streams, one from the north associated with the cold surge and the other from the northeast associated with the trade winds north of South America. This same confluence was seen in the cold surge associated with SS93 (Schultz et al. 1997, Fig. 5a). Also at day $+3$, the equatorward advance of the anticyclone continued, strengthening the trade winds by 2–6 m s^{-1} across 60° of longitude from Costa Rica to 140°W (Fig. 7d). This strengthening of the trade-wind belt at low latitudes after the arrival of cold surges has been discussed by Riehl (1954, 273; his ''surges of the trades''); he noted that the trade-wind surges can last for several days and span thousands of kilometers as wind speeds increase to 15–25 m s^{-1}. For the cold surge associated with SS93, the surface winds in the ECMWF analysis increased up to 10 m s^{-1} along 20° of longitude (90°–110°W) over the eastern Pacific (Schultz et al. 1997, their Figs. 2a, 9b). Chang et al. (1979) have also noted strengthened lower-tropospheric northeasterlies in the Tropics associated with east Asian cold surges.

c. COOL

The 200-hPa streamfunction anomalies in COLD differ from those in COOL in that a cyclonic anomaly preexisted over the southeast United States and a larger area of anticyclonic anomalies was found over the east-

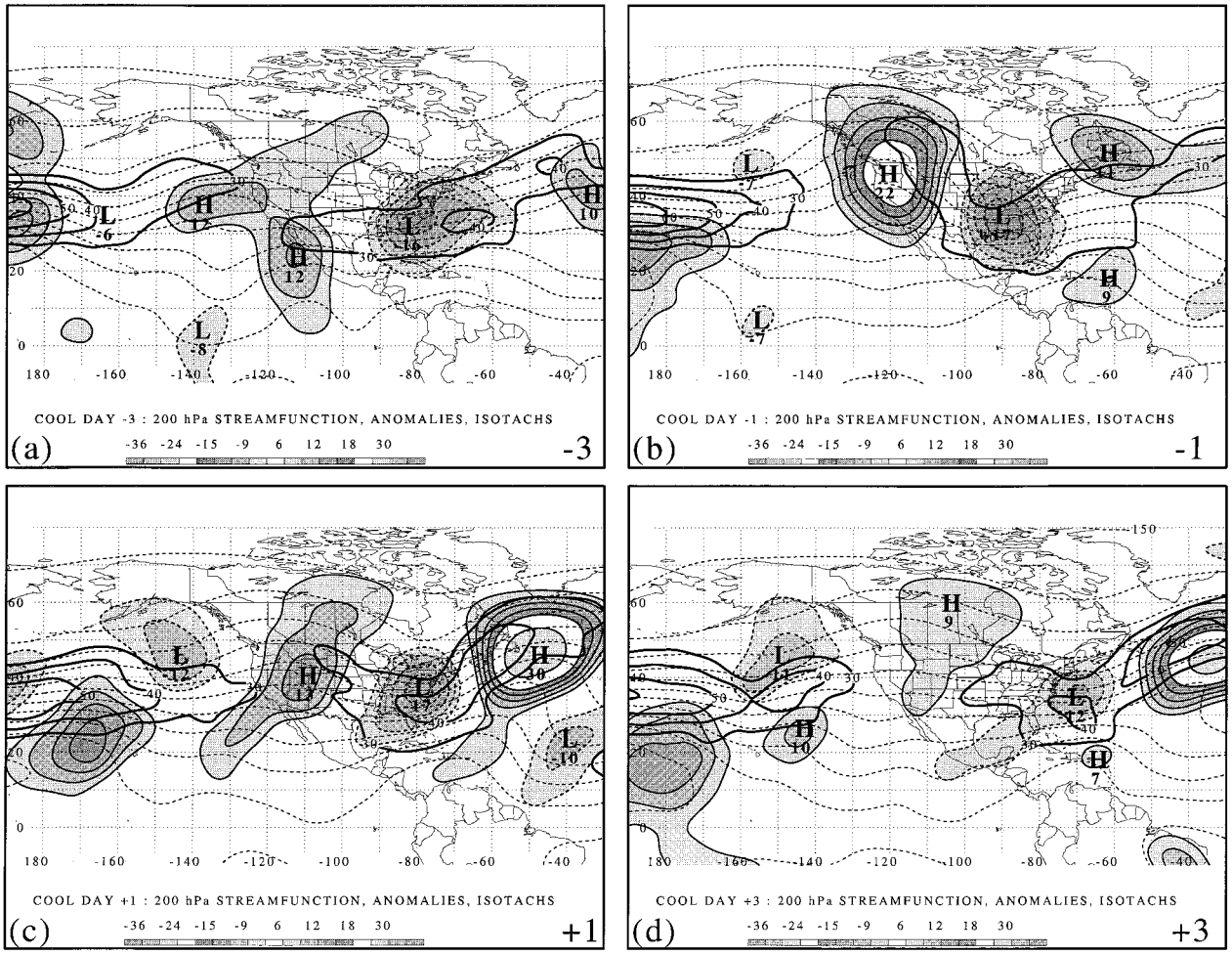

FIG. 8. As in Fig. 4 except for COOL.

ern North Pacific in COOL at day −3 (cf. Figs. 4a to 8a). This pattern resulted in the upper-level flow over northern Mexico and the Gulf of Mexico being weaker, more zonal, and less confluent than in COLD. By day −1, a deepening trough over the Mississippi Valley was apparent and a broader, higher-amplitude ridge in the western United States was present compared to COLD (cf. Figs. 4b to 8b). After the surge onset, the amplitude of the ridge in COOL weakened considerably compared to the nearly constant amplitude maintained by the anticyclonic anomaly in COLD (cf. Figs. 4c,d to 8c,d). Also, the trough in the eastern United States was much farther north and east in COOL relative to that in COLD (cf. Figs. 4c,d to 8c,d). This flow evolution meant that there was less inferred dynamical forcing for the equatorward movement of the cold air and lower-tropospheric anticyclone because (a) the absence of the 200-hPa confluence meant the absence of the lower-tropospheric ageostrophic northerlies in eastern Mexico that would aid in the equatorward movement of cold air, (b) the rapid collapse of the western United States ridge inhibited further support for the anticyclone from higher latitudes, and (c) the more northward and eastward motion of the eastern United States cyclone favored the quick advance of the cold air away from the Tropics.

At day −3, two 1000-hPa anticyclonic height anomalies were present in COOL (Fig. 9a): one over eastern Mexico (not statistically significant) and another offshore of northern California associated with the 200-hPa anticyclonic anomaly exiting the Pacific jet (Fig. 8a). The anomaly in Mexico was related to previous surges, as Table 3 indicates in five out of the eight cases that this composite comprises (explaining why this anomaly was not statistically significant) occurred within five days of a previous cold surge. The presence of higher heights (and cooler air; see Fig. 10a) in Mexico therefore mitigated any large temperature decreases from later surges [also noted by Mecikalski and Tilley (1992)]. Likewise, the arrival of the anticyclone from the eastern Pacific (as opposed to central Canada as occurred in COLD) would bring cooler air, likely of Pacific origin (as opposed to much colder continental/arctic air), equatorward (cf. Figs. 5a,b to 9a,b). The center of the anticyclone in COOL moved from the

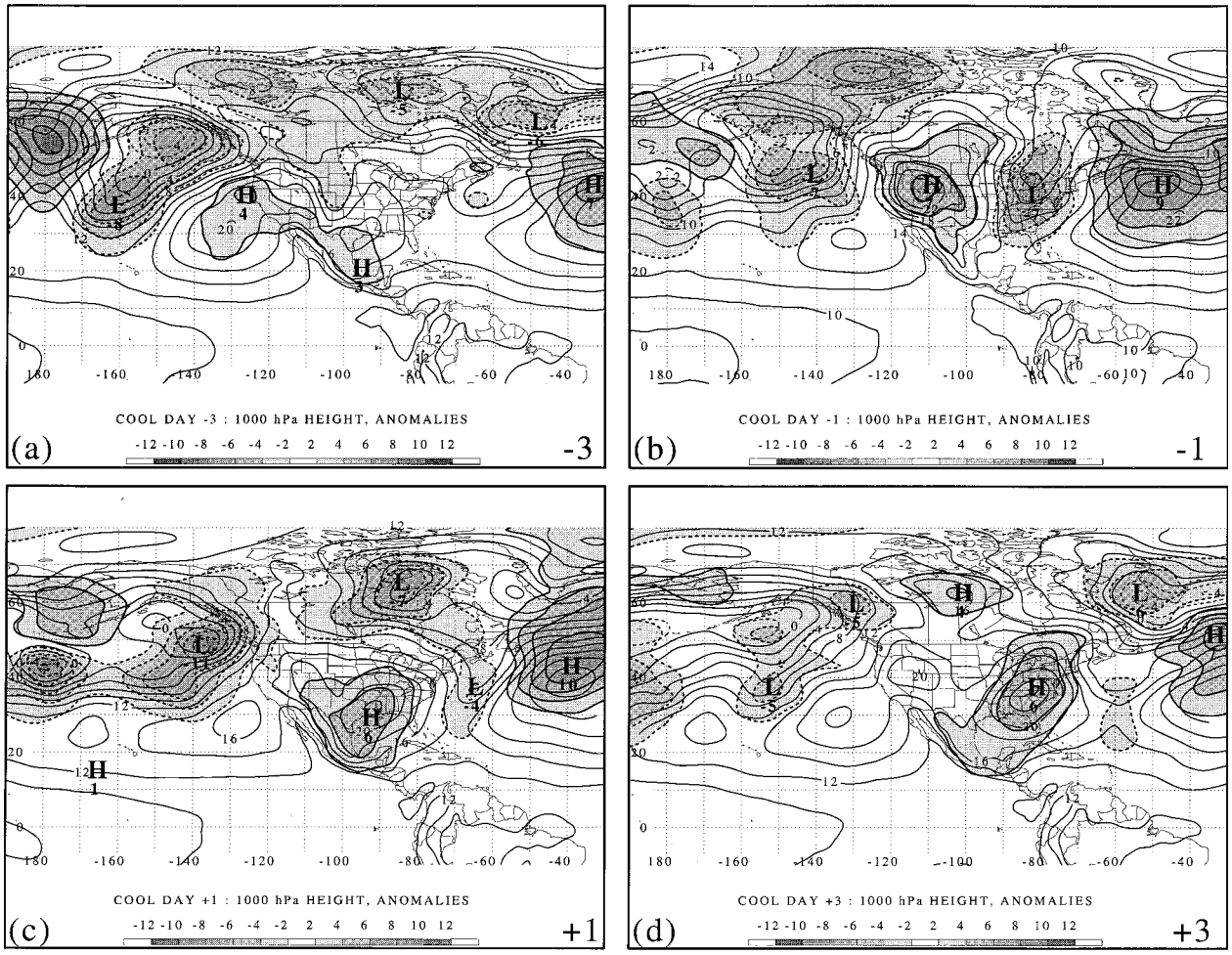

FIG. 9. As in Fig. 5 except for COOL.

North Pacific Ocean, over the mountains of western Wyoming and Colorado, into the southeast United States, and up along the Appalachians (Figs. 9a–d), similar to the tracks of orographically modified anticyclones discussed by, among others, Klein (1957), Hsu (1987), and Wallace et al. (1988). Compare the track in Figs. 9a–d to that of the composite anticyclone in COLD, which originated east of the Canadian Rockies and moved equatorward along the mountains into Central America (Figs. 5a–d). The trailing ridge in Mexico and Central America in COOL (Fig. 9d) is further evidence of orographic channeling, even for surges with weaker temperature contrasts.

The 850-hPa temperature anomalies for COOL are shown in Fig. 10. A major difference between the COLD and the COOL composites is the near absence of anomalously cold air in Canada in the COOL cases (cf. Figs. 6a to 10a). As noted earlier, previous cold-surge events in some of the cases comprising COOL resulted in below-normal temperatures in the southeast United States and Gulf of Mexico (Fig. 10a). The cold anomaly, associated with northerly flow between the lower-tropospheric cyclone and anticyclone (e.g., Fig. 9b), was centered over Iowa at day −1, reached the Carolinas by day +1, and eventually moved off the east coast of the United States (Figs. 10b–d). The 850-hPa cooling in Mexico and Central America amounted only to 2°–4°C compared to up to 10°C in COLD (cf. Figs. 6d to 10d). The thermal ridge downstream of the cold surge was of much higher amplitude than that in COLD (cf. Figs. 6c,d to 10c,d) and appeared to be associated with the stronger East Coast cyclogenesis in COOL (Fig. 9c,d).

The 850-hPa anticyclonic streamfunction anomaly responsible for the cold surge originated over the eastern North Pacific and maintained its intensity as it moved onshore compared to the rapid amplification over western North America of the corresponding anomaly in COLD (cf. Figs. 7a,b to 11a,b). Other notable differences between COLD and COOL include the hyperbolic deformation zone over the Caribbean in COOL being farther east than in COLD, acting to draw the cold air farther east, and the postsurge increase in the trade winds over the eastern North Pacific being less im-

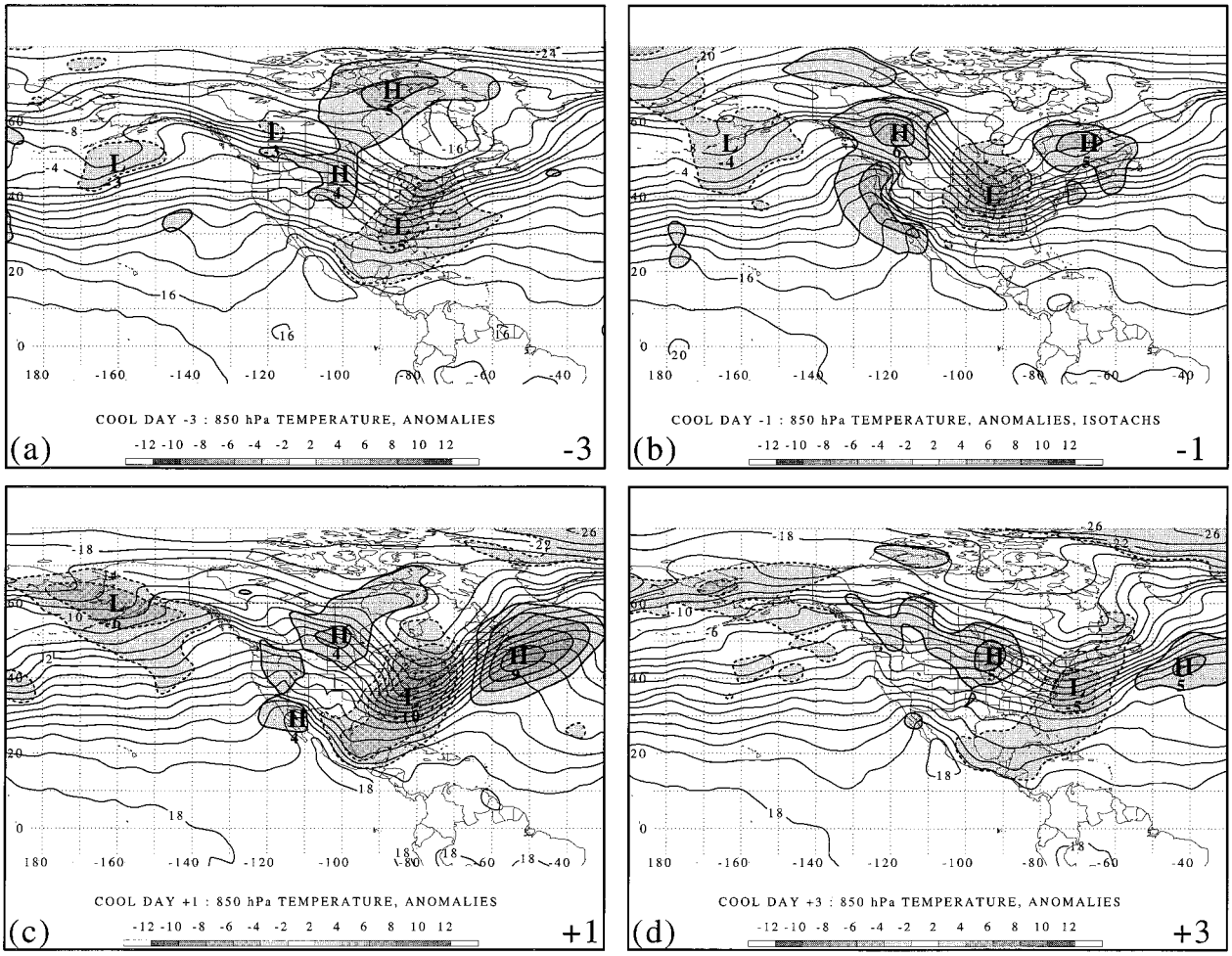

FIG. 10. As in Fig. 6 except for COOL.

pressive (0–2 m s^{-1}), but a bit more zonally extensive along 150°–160°W (cf. Figs. 7c,d to 11c,d).

d. HIGH

The HIGH composite, composed of cold surges that do not reach low latitudes, is qualitatively similar to climatology with a weak ridge over the western United States and a trough over the eastern United States (not shown); anomalies are relatively small at all levels. The HIGH composite appears to be a less amplified version of the COOL composite with the ridge over the western United States rapidly weakening after day −1. The similarity of HIGH to climatology implies that cold-frontal passages into central Mexico can be rather common (section 2b), but their advance farther equatorward into Central America is a less frequent occurrence since the higher-amplitude flows characteristic of COLD and COOL surges are less likely to occur.

e. LONG

Figure 12 shows the LONG composite and anomaly fields for day −3. Long-duration events are not necessarily characterized by high-amplitude, anomalous upper-level flows as the magnitudes of most of the anomalies are smaller than those in COLD or COOL (cf. Figs. 4a and 8a to 12a). LONG events also appear to be aided by larger areas of anticyclonic anomalies and weaker cyclonic anomalies throughout the lower troposphere over much of the eastern North Pacific Ocean compared to COLD or COOL (cf. Figs. 5a, 7a, 9a, and 11a to 12b,d). The anticyclonic anomalies exhibit less vertical tilt compared to similar anomalies in the COLD and COOL cases, likely indicating more barotropic, slower-moving, and slower-evolving features (in 8 days, the western United States ridge progressed only 30° of longitude) (cf. Figs. 12a to 13a), results consistent for long-duration cold surges over the eastern Mediterranean region (Saaroni et al. 1996). The 1000-hPa anticyclone associated with the cold surge origi-

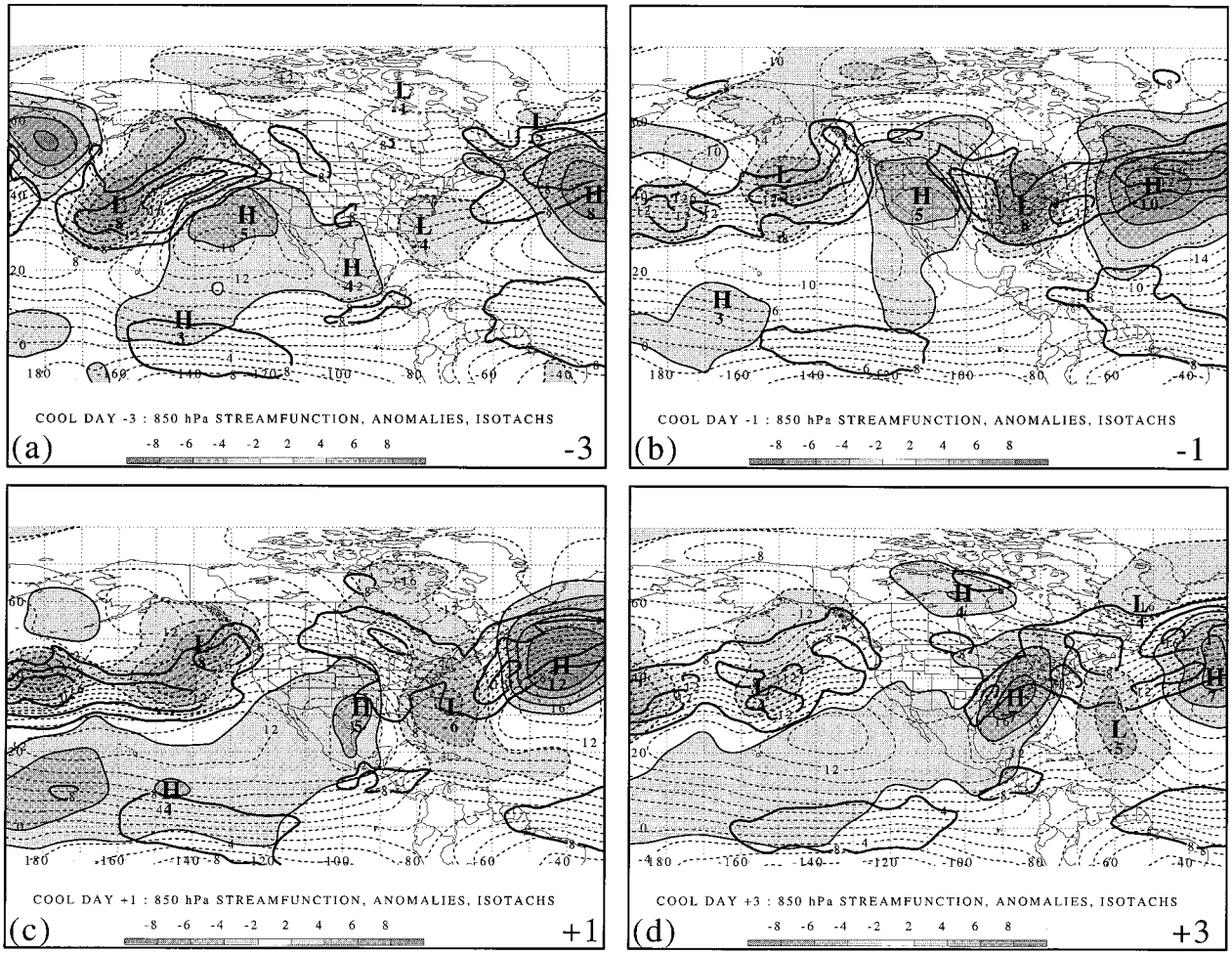

FIG. 11. As in Fig. 7 except for COOL.

nates from over the eastern North Pacific Ocean, indicating that extremely cold, continental arctic air is usually not associated with long-duration surges (Figs. 12b,c), in agreement with Fig. 1 and the modest average ΔT (6.6°C) in Table 4.

After the onset of the surge and approximately midway through the duration of the event (day +5), the 1000-hPa anticyclone associated with the cold surge has taken a track similar to that in COOL (cf. Figs. 9a–d to Figs. 12b, 13b). Confluence at 200-hPa (stronger than in COOL, but not as strong as in COLD; cf. Figs. 4a to 8a) over the Gulf of Mexico has developed during this 8-day period (cf. Figs. 12a to 13a), helping to maintain the high 1000-hPa heights over Mexico and the southern United States (Fig. 13b). Temperatures at 850 hPa over Mexico have decreased, whereas anomalously high temperatures in the lee of the mountains in the central United States and Canada occurred where southwesterly flow at 850 hPa has promoted lee troughing (Figs. 13c,d). The 1000-hPa height at day +5 indicates that another anticyclone centered over Colorado will head equatorward and continue to support anomalously high heights over northern Mexico (Fig. 13b). As such, it appears that long-duration events are sometimes characterized by multiple surges from the United States, which maintain anomalously anticyclonic flow over eastern Mexico [e.g., Mecikalski and Tilley (1990, 260); Colle and Mass (1995, Fig. 3, −48 h)]. For example, during one of Reding's (1992) long-duration events (D = 10 days, onset date: 21 January 1989), the time series of wind speed from the central Gulf of Tehuantepec was available owing to moored instrumentation obtained during Tehuano, an oceanographic field program (Trasviña et. al. 1995, Fig. 3). Although the wind speed in the Gulf of Tehuantepec, while a convenient surrogate, may not be directly related to the duration of the surge, the single-surge event (as defined by Reding) of 21–31 January 1989 actually consisted of three separate wind events, each exceeding 8 m s^{-1}, interspersed with calm periods.

Even if a CACS episode ends, the large-scale flow pattern may remain nearly steady with the planetary-scale anomalies in the appropriate locations to favor further cold surges. To this end, the LONG composite

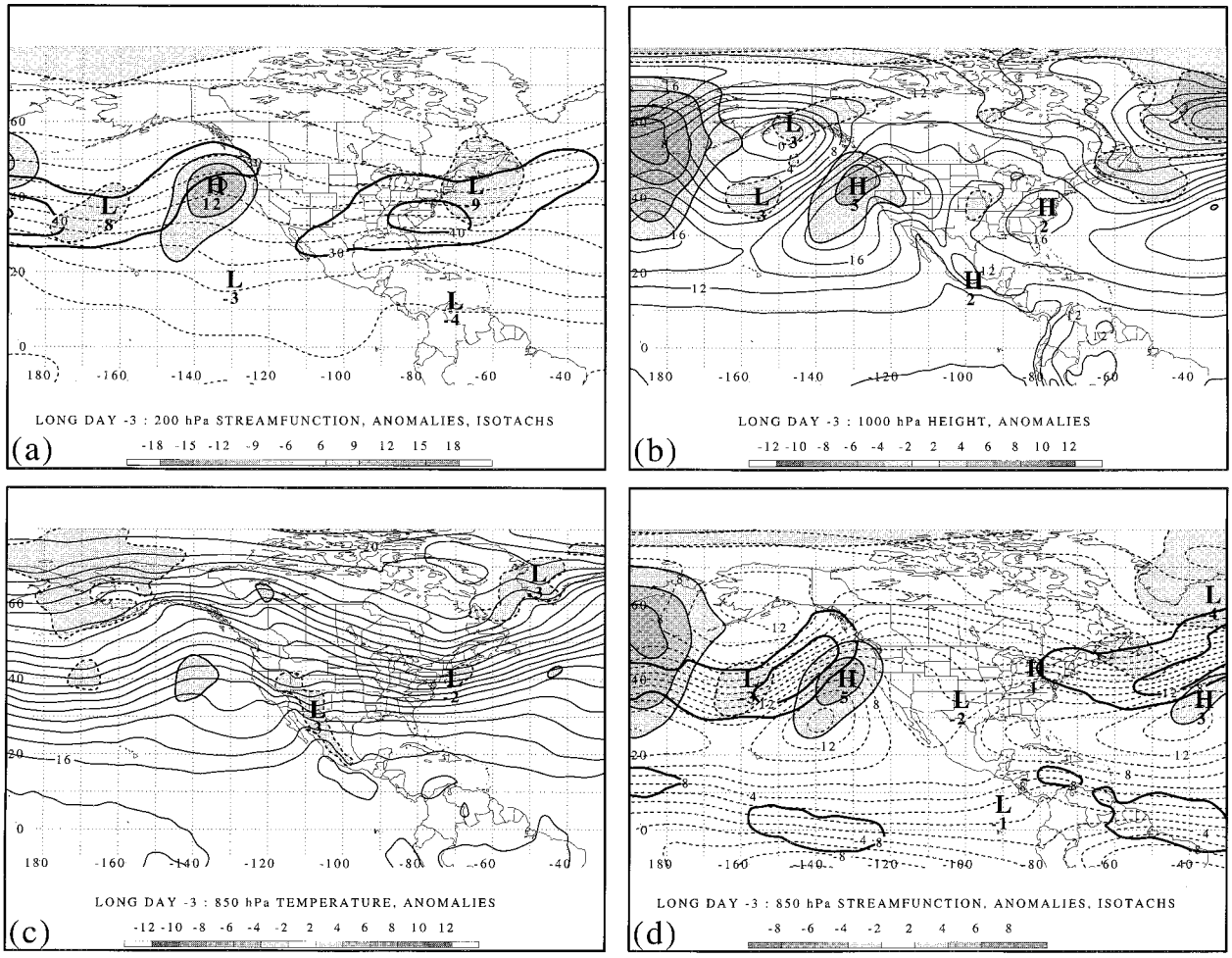

FIG. 12. LONG day −3: (a) 200-hPa composite streamfunction (thin dashed lines every 15 × 10^{-6} m^2 s^{-1}), streamfunction anomalies from weighted climatology [×10^{-6} m^2 s^{-1}, contoured and shaded according to scale at bottom of figure; solid (dashed) lines surround positive (negative) values], 200-hPa composite isotachs of total horizontal wind (thick solid lines every 10 m s^{-1} starting at 30 m s^{-1}). (b) 1000-hPa composite geopotential height (solid lines every 2 dam), geopotential height anomalies from weighted climatology [dam, contoured and shaded according to scale at bottom of figure; solid (dashed) lines surround positive (negative) values]. (c) 850-hPa composite temperature (solid lines every 2°C), temperature anomalies from weighted climatology [°C, contoured and shaded according to scale at bottom of figure; solid (dashed) lines surround positive (negative) values]. (d) 850-hPa composite streamfunction (thin solid lines every 2 × 10^{-6} m^2 s^{-1}), streamfunction anomalies from weighted climatology [×10^{-6} m^2 s^{-1}, contoured and shaded according to scale at bottom of figure; solid (dashed) lines surround positive (negative) values], 850-hPa composite isotachs of total horizontal wind (thick solid lines every 4 m s^{-1} starting at 8 m s^{-1}).

resembles a less amplified version of Lackmann et al.'s (1996, Figs. 9a–g) composite for temporally clustered, western North Atlantic cyclogenesis in which the ridge over the western United States moves slowly eastward. A cursory examination of Reding's cases suggests that clustering of cold-surge events can occur and is not uncommon (not shown). Hill (1969, chapter 4), Henry (1979, 1079), Boyle (1986a, 917), and Chang and Chen (1992) also recognized that cold surges showed the potential for clustering with the individual events of the cluster possessing similar properties. For the 39 cases in Colle and Mass (1995, Table 1), the time between successive surges was 10 days or less for six pairs of events. These facts suggest that clustering of cold surge events to extend the duration of an existing CACS (LONG) or to have repeated CACSs occur within a short period of time is possible.

The conditions that bring about the end of a long-duration event are investigated using the composite LONGC (not shown) and are similar to those that bring about the end of shorter duration events: a short-wave trough approaches the western United States and begins to reform over the central United States (e.g., Steenburgh and Mass 1994; Colle and Mass 1995) or northern Mexico (Schultz et al. 1997), lowering the heights, and allowing the eastward migration and/or dissipation of the anticyclone. These results indicate that the unique aspect about LONG is not the occurrence of an unusual

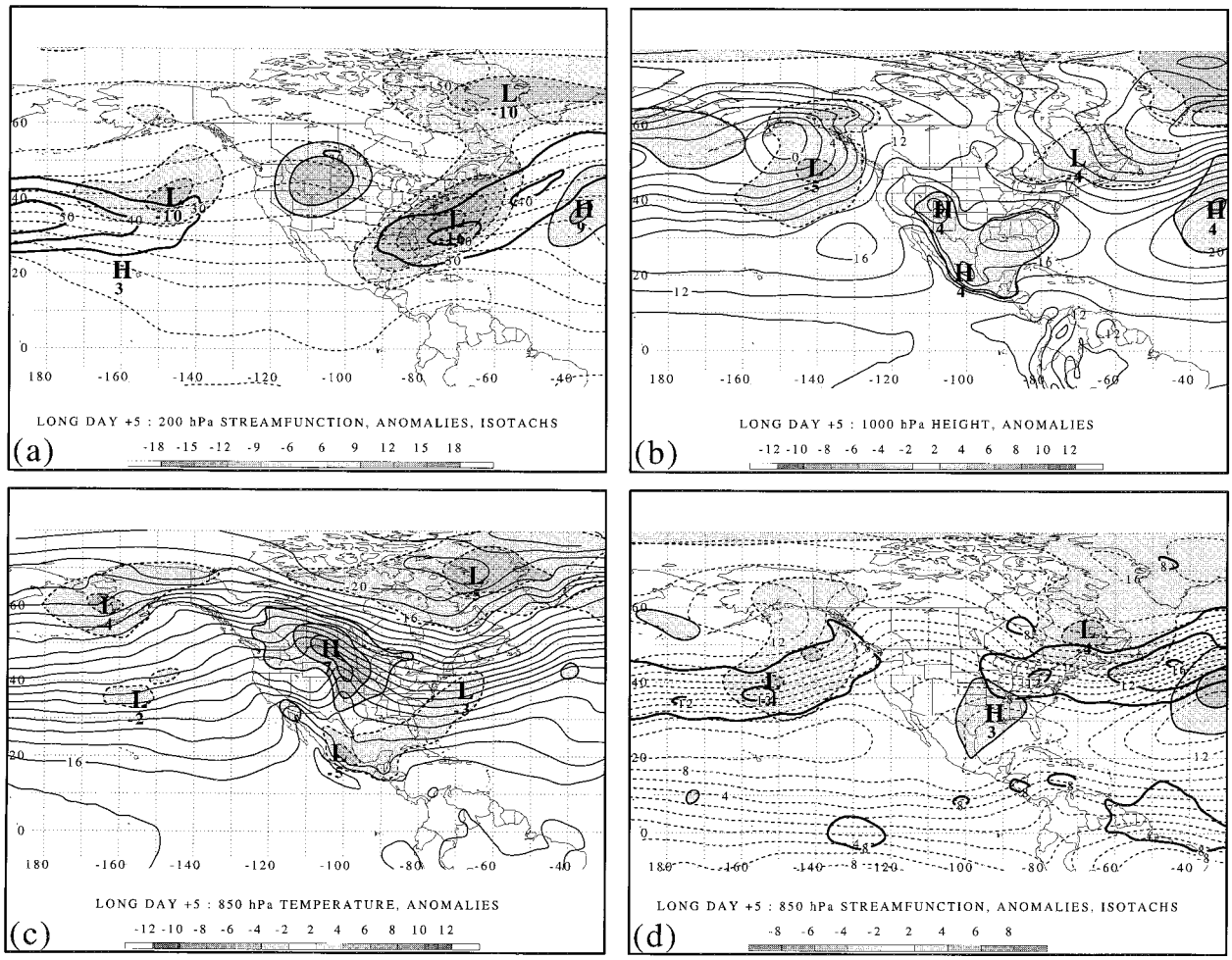

FIG. 13. As in Fig. 12 except for day +5.

event that causes long-duration surges to end, but the occurrence of one or more rather ordinary conditions, which cause the long-duration surge to be maintained: a slower-moving planetary-scale pattern, the presence of multiple surges to reinforce the event, and the absence of mobile short-wave troughs at relatively low latitudes.

f. Discussion

Although the topography of the Rocky Mountains and the Sierra Madre undoubtedly plays an important role in the channeling of cold surges equatorward (e.g., Hartjenstein and Bleck 1991; Colle and Mass 1995), differing planetary- and synoptic-scale flow patterns can also be conducive to the intensity and longevity of CACSs. Although the dynamics of the leading edge of a cold surge occur on the mesoscale (Colle and Mass 1995; Schultz et al. 1997), specific conditions need to be satisfied on much larger scales in order to support the equatorward advance of the cold surge. Generally, the composite results from this section are broadly similar to those from other studies of cold surges in North America (e.g., Dallavalle and Bosart 1975; Boyle and Bosart 1983; Konrad and Colucci 1989; Mecikalski and Tilley 1992; Colle and Mass 1995; Garcia 1996; Konrad 1996; Schultz et al. 1997).

The intensity of the surge (as measured by the most equatorward extent and the temperature drop behind the surge) appears to be related to two factors: a persistent, narrow, high-amplitude 200-hPa ridge over the western United States and 200-hPa confluence over the Gulf of Mexico (e.g., Figs. 4 and 14a). As shown by Dallavalle and Bosart (1975) and Boyle and Bosart (1983), the persistence and narrowness of the ridge ensure that upper-level anticyclonic vorticity advection (and associated lower-tropospheric height rises) on the eastern flank of the ridge favors the equatorward movement of the lower-tropospheric anticyclone. Poleward of the confluent jet-entrance region is upper-level convergence, which is associated with strong subsidence over the low-level anticyclone. Strong low-level northerlies associated with the direct secondary circulation at the jet-entrance region enhance the cold advection into low latitudes. That the more intense surges (COLD) tend to

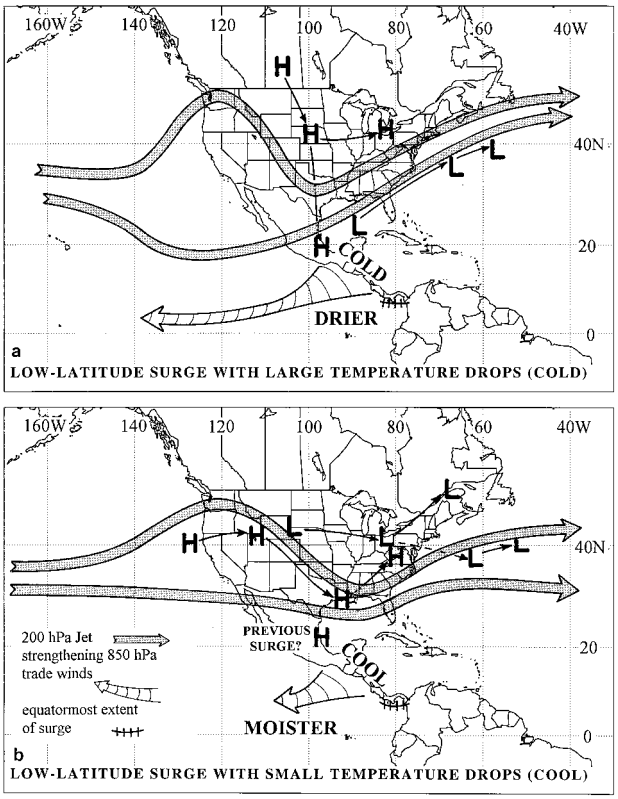

FIG. 14. Comparing (a) COLD vs (b) COOL surges. Here, H (L) represents track of surface anticyclone (cyclone) center(s) approximately every two days. Other symbols are defined in the legend in (b).

occur later in the cold season (cf. Tables 2 and 3) when the subtropical jet stream is stronger (H. Iskenderian 1996, personal communication) is consistent with the above argument. In contrast, the COOL surges have a progressive, broad ridge over the western United States and much weaker confluence, so the dynamical forcing for the lower-tropospheric anticyclone is not as strong (Figs. 8 and 14b). These results are consistent with those of Chang and Lau (1982) and Lau et al. (1983), who show that stronger east Asian cold surges occur when the North Pacific jet-entrance region is intensifying and becoming increasingly more confluent. Without strong upper-level dynamics associated with COLD surges, strong cooling behind the surge is not likely. Nevertheless, even with moderate forcing, the leading edge of COOL surges can still reach 7°–9°N. This would seem to indicate that the topography must be playing a role to assist the low-latitude extent of both COLD and COOL surges.

Another factor that distinguishes COLD from COOL surges is the path of the low-level cyclone and anticyclone. Cyclogenesis in the Gulf of Mexico usually is coincident with the movement of the surge equatorward in the COLD cases, whereas Colorado lee cyclogenesis typically precedes the surge in COOL by about two days (cf. Figs. 5–9 to Figs. 14a, b). For COLD surges, the anticyclone associated with the cold surge originates east of the Canadian Rockies. The anticyclone remains close to the Rockies as it heads equatorward and, therefore, the brunt of the cold arctic air will be felt in Mexico and Central America (Figs. 5 and 14a). In contrast, COOL surges tend to be associated with anticyclones that arrive from over the eastern North Pacific Ocean and are associated with milder maritime air (Figs. 9 and 14b). The anticyclone crosses the intermountain west and moves into the southeast United States. In these cases, the coldest air behind the cyclone generally moves eastward, not equatorward into Central America. Klein (1957, 14, 58–60) recognized these two distinct anticyclone tracks over North America (those from the continental polar regions and from the Pacific). In addition, the existence of a prior surge to COOL can help to reduce the temperature decrease associated with the surge (cf. Tables 2 and 3).

In contrast to the moderate to strong upper-level dynamics present in the COOL and COLD cases, much weaker upper-level forcing is present in the HIGH composite. HIGH surges do not reach equatorward of Honduras and are associated with progressive and small-amplitude anomalies that are not significantly different from climatology. Since the upper-level dynamics are much weaker, equatorward migration of the cold surge is likely to be more dependent upon the interaction with topography. In an attempt to isolate the impact of topography upon the cold surge, Colle and Mass chose their case study (13 November 1986) based on the fact that there was weak low-latitude dynamic forcing. Indeed, the flow aloft was neither strong nor confluent (Colle and Mass 1995, Figs. 5c, 6c, 7c, and 8c). This cold surge did not reach MID (B. A. Colle 1995, personal communication) and, consequently, was not classified as a cold surge in Reding's listing of CACS events. In fact, the 13 November 1986 event was the only case in the Colle and Mass (1995) climatology that did not result in a CACS as defined by Reding (1992), suggesting that upper-level dynamic forcing, through either a properly situated low-latitude trough, a confluent jet-entrance region over the Gulf of Mexico, or both, is necessary to have a cold surge reach equatorward of 20°N. Therefore, it might be appropriate to consider a spectrum of cold surges that ranges from those that are primarily topographically forced given certain synoptic conditions (the 13 November 1986 event of Colle and Mass) to those that are more dynamically forced on the planetary and synoptic scales [e.g., the cold surge associated with SS93 (Schultz et al. 1997)], with most cold surges a result of both forcings.

These results are broadly consistent with previous classifications of cold surges in the Americas. Frankenfield (1917) identified four sea level pressure patterns that preceded wind events in Panama. The COLD composite, with its Gulf of Mexico cyclogenesis and anticyclone originating from south-central Canada, resem-

bled his first type. His other three types, with characteristics such as a Pacific anticyclone, central plains cyclogenesis, and a southeast United States anticyclone, resemble different stages in the COOL composite. Hill (1969) found two types of cold-frontal passages in Mexico: northern-type (resembling the COLD cases) and Pacific-type (resembling the COOL cases). Henry (1979) noted that cold fronts at the leading edge of an anticyclone originating from continental arctic or continental polar regions over North America (as in COLD) are generally oriented west-southwest–east-northeast by the time they arrive over the Gulf of Mexico and have a better chance of carrying the bulk of the cold air farther equatorward than cold fronts coming from the Pacific Ocean, which are primarily oriented south-southwest–north-northeast (as in COOL). Crisp and Lewis (1992) classified anticyclones that reached the Gulf of Mexico into those bearing continental polar air (resembling the COLD cases) and those bearing maritime polar air (resembling the COOL cases). Mecikalski and Tilley (1992) proposed a classification scheme for cold surges based on where the anticyclone originated: northern class (resembling the Canadian anticyclones of COLD) and western class (resembling the Pacific anticyclones of COOL and HIGH). The northern class was further subdivided (NA and NB) based on the path of the anticyclone center and the most equatorward extent of the leading edge of the cold surge. A type NA cold surge is defined as a northern-class cold surge in which the center of the anticyclone moved south of 40°N and the leading edge of the surge moved south of 25°N; this type resembles the COLD composite. A type NB cold surge is defined as a northern-class cold surge in which the center of the anticyclone reached between 40° and 50°N, but the leading edge did not reach 25°N. Type NB would most closely resemble the HIGH composite, except the anticyclone originated over Canada (NB) as opposed to the Pacific (HIGH). And finally, Konrad (1996) discriminated between extreme and moderate cold-air outbreaks over the southeastern United States. He found that extreme outbreaks were characterized by a Canadian anticyclone, East Coast cyclogenesis, and high-amplitude 500-hPa flow, consistent with the COLD composite, whereas the moderate outbreaks were characterized by a North Pacific anticyclone, below-normal temperatures in the southeast United States prior to the outbreak (suggesting a previous outbreak), an eastward-moving central United States cyclone, and lower amplitude 500-hPa flow, consistent with the COOL composite. Additionally, these results are also consistent with Wu and Chan (1995, 1997), who identified northerly and easterly surges at Hong Kong (similar to our COLD and COOL, respectively). Much previous work has discussed the relationships between east Asian cold surges and winter monsoon circulations [see Boyle and Chen (1987) and Lau and Chang (1987) for reviews]. The paradigm that is emerging from this body of research is of the acceleration of air at upper-levels into the North Pacific jet stream entrance region, favoring strong east Asian cold surges. A local enhancement of the Hadley and Walker circulations result, which is related to an increase in the northeast trade winds (e.g., Chang et al. 1979), enhanced lower-tropospheric convergence and convection (e.g., Chang and Lau 1980; Lau 1982; Lau et al. 1983; Chu and Park 1984; Chang and Lum 1985; Chang and Chen 1992; Wu and Chan 1997), westerly wind bursts (e.g., Love 1985; Chu 1988), and increased upper-level divergence, which further strengthens the jet and leads to downstream development (e.g., Ramage 1968; Joung and Hitchman 1982; Lau et al. 1983; Lau and Chan 1983; Boyle 1986b). While we have presented evidence for some of these relationships in CACSs [e.g., the increasing confluence in the jet-entrance region over the Gulf of Mexico (Fig. 4), the increase in the northeast trade winds in (Fig. 7), and the amplification of troughs and ridges downstream of the cold surge in a manner analogous to downstream development (Figs. 4 and 8)], the inability of the ECMWF analyses to adequately resolve tropical convection and its divergence (Hoskins et al. 1983, 1610–1611; Trenberth and Olson 1988; Trenberth 1992, 8–12, 26–34) makes it difficult to convincingly document the existence of these feedbacks in our composites. Therefore, further research is required to draw additional parallels between east Asian and Central American cold surges.

4. Relationship of Central American cold surges to El Niño–Southern Oscillation

As illustrated in the previous section (e.g., Fig. 14a), strong cold surges in Mexico and Central America usually possess a positive Pacific–North American pattern and confluent subtropical jet over the Gulf of Mexico and southeast United States. These features are also found during El Niño conditions (e.g., Douglas and Englehart 1981; Horel and Wallace 1981; Arkin 1982; Gray 1984; Aceituno 1989; Cavazos and Hastenrath 1990). Therefore, it might be expected that an anomalously large number of strong cold surges into Mexico and Central America would occur during El Niño years when the confluent jet-entrance region is more likely to be present over the Gulf of Mexico.

To examine this hypothesis, Fig. 15 presents a 60-yr record of the number of cold surges in southern Mexico [based on data in Klaus (1973, 111–112)] showing a large degree of interannual variability ranging from 0 to 27 events per cold season (September–April). With an average of 13 events per cold season, these data are comparable to values found in this (section 2b) and other studies (e.g., Hill 1969; DiMego et al. 1976; Henry 1979; Horvath and Henry 1980; Reding 1992). Table 5 shows that the cold season following an El Niño year is likely to have about twice the number of cold-frontal passages than the cold season following a La Niña year (14.6 versus 7.5), results consistent with those of Yarnal

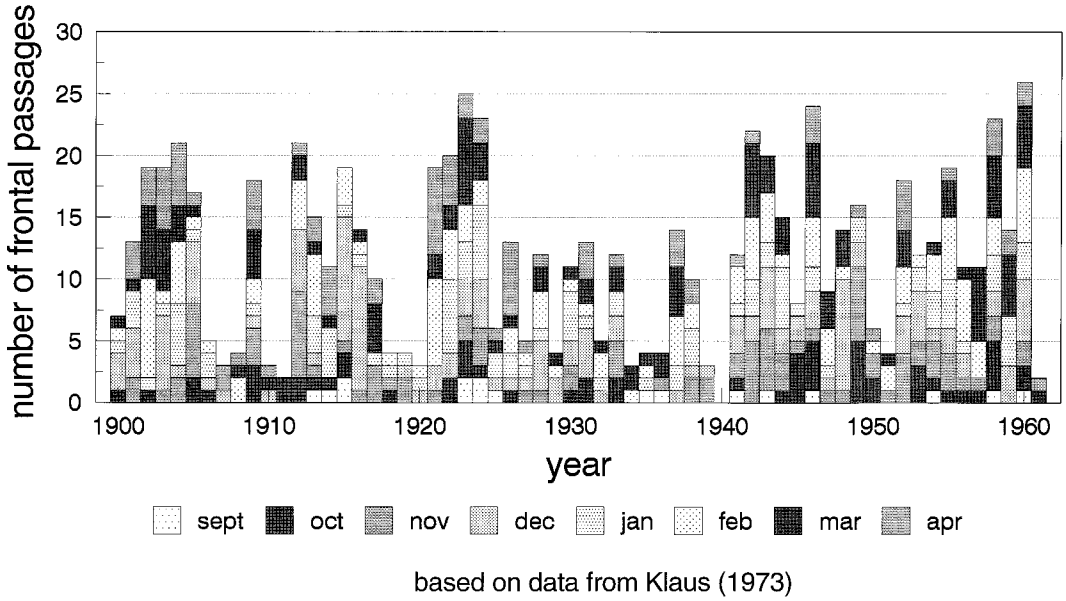

FIG. 15. Number of cold-frontal passages per month in the southern Mexico region during the cold season (September–April) for 1899–1900 (under column labeled ''1900'') through 1959–60 (under column labeled ''1960'') and October–November 1960 (under column for ''1961''). Prepared from tabular data presented in Klaus (1973, 111–112). (Figure courtesy of A. Seimon.)

TABLE 5. Number of cold-frontal passages in southern Mexico for a given calendar year (January–December) and for the following cold season (September–April) based on data presented in Klaus (1973, Table 2). For example, ''next cold season'' of 1900 means September 1900–April 1901. Years are defined as ''El Niño'' (N = number of years = 17) of ''La Niña'' (N = 11) (Halpert and Ropelewski 1992, Tables 1 and 2, respectively).

	Number of cold fronts			Number of cold fronts	
El Niño year	Calendar year	Next cold season	La Niña year	Calendar year	Next cold season
1900	9	13	1904	43	21
1905	6	17	1909	12	3
1911	14	21	1910	4	2
1912	11	15	1915	15	14
1914	24	19	1917	14	4
1918	5	4	1924	15	6
1919	2	3	1928	9	4
1923	30	23	1938	11	3
1925	6	13	1950	3	4
1930	12	13	1955	17	11
1932	11	12	1956	9	11
1940	7	12			
1941	12	22			
1946	17	9			
1951	10	17			
1953	9	13			
1957	18	23			
Average	11.9	14.6	Average	13.8	7.5
Std dev	6.9	5.8	Std dev	10.1	5.7

and Diaz (1986). On the other hand, the phase of ENSO appears to have little effect on the number of cold-frontal passages in a given *calendar year* (Table 5). There is also substantial variability in the number of cold surges that occur in non–El Niño or non–La Niña years (Fig. 15), indicating that the phase of ENSO is not the only factor that affects the number of frontal passages [also noted by Yarnal and Diaz (1986)].

These results relating ENSO to the number of cold surges are consistent with previous research. For example, the cold season following an El Niño year (conditions favorable for an above-average number of cold surges) would be characterized by below-normal temperatures over the southeast United States due to the repeated cold surges, results in agreement with those of Halpert and Ropelewski (1992). In addition, cold surges tend to produce a greater acceleration of the trade winds over the eastern North Pacific Ocean (Figs. 7d and 11d). Therefore, El Niño years with an above-average number of cold surges would result in generally stronger trade winds, a process that Bjerknes (1969) and Wyrtki (1975) have noted as playing an integral role in ENSO. In addition to producing surface temperature and wind anomalies, a large number of cold surges would imply that the regions of Mexico and Central America that are favorable for orographic precipitation would be wetter than normal. While many studies have shown correlations between ENSO and annual precipitation in North and Central America (e.g., Estoque et al. 1985; Hastenrath et al. 1987; Ropelewski and Halpert 1987; Rogers 1988; Cavazos and Hastenrath 1990; Waylen et al.

1994; Waylen et al. 1996a; Stone et al. 1996; Enfield 1996), they do not possess the small temporal and spatial scales necessary to address this question adequately. Waylen et al. (1996b) examined monthly precipitation at 105 stations in Costa Rica and found that the precipitation at stations in eastern (western) Costa Rica was negatively (positively) correlated to the Southern Oscillation index (i.e., El Niño years were wetter east of the mountains and drier west of the mountains). These results are consistent with similar findings for Panamanian rainfall and ENSO (Estoque et al. 1985) and are also consistent with our hypothesis.

This study therefore indicates that the nature of the planetary- and synoptic-scale flow during the cold season is an important factor to the intensity and number of cold surges, in agreement with previous studies from North America, Central America, and east Asia. This work also suggests that cold surges can affect the tropical atmosphere and ocean through increasing the strength of the trade winds, which are related to ENSO as we have argued. Therefore, cold surges can be employed as a surrogate to illustrate interannual climatic variability and can be considered integral to the global circulation.

5. Summary

Based on a previous case study, we examined the factors that affected the intensity and longevity of Central American cold surges using an 11-cold-season climatology of cold surges (Reding 1992). Strong cold surges (defined as those reaching low-latitudes and bearing large temperature decreases) were distinguished from weaker cold surges by a confluent 200-hPa jet-entrance region over Mexico and the Gulf of Mexico, a high-amplitude persistent ridge over the western United States, and differing origins and paths of the anticyclone responsible for the cold surge (arctic versus Pacific origin). Long-duration events are characterized by a slower-moving planetary-scale flow pattern, multiple surges that reinforce the event, and the absence of mobile shortwave troughs at low latitudes. In addition, cold surges tended to be more numerous during the cold season after an El Niño year, consistent with the prevalence of the the low-latitude jet-entrance region. This work suggests that additional research to investigate planetary- and synoptic-scale flow patterns favorable for cold surges associated with abundant or sparse precipitation (e.g., Bosart and Schwartz 1979) may be useful. These composites could then be related to the numerous studies of precipitation patterns associated with ENSO.

Acknowledgments. We are deeply indebted to the following individuals for their contributions to this work: Dr. Haig Iskenderian of Atmospheric and Environmental Research, Inc. for assistance in obtaining ECMWF analyses and for sharing his work on the subtropical jet stream; Greg Hakim of the University at Albany, State University of New York (SUNYA) for his comments, which substantially improved the compositing technique; Anton Seimon of SUNYA for kindly providing Fig. 15; Prof. James McGuirk of Texas A&M University for generously providing a copy of Reding (1992); Dr. David Fitzjarrald of SUNYA for providing relevant references on cold surges; Prof. Michael Richman of the University of Oklahoma, Dr. Armando Trasviña of the Centro de Investigación Científica y de Educación Superior de Ensenda, Dr. Guillermo Quiros Alvarez of the Oceanography and Coastal Management Laboratory of the Universidad Nacional de Costa Rica, Prof. Peter Waylen of the University of Florida, Prof. James Steenburgh of the University of Utah, and Dr. David Enfield of the National Oceanic and Atmospheric Administration (NOAA) Atlantic Oceanographic and Meteorological Laboratories for their advice and interest in this project; Marilyn Peacock of SUNYA for drafting some of the figures; and Dr. Brian Colle of the University of Washington, Dr. Michael Douglas of the National Severe Storms Laboratory (NSSL), and the anonymous reviewers for comments that improved the presentation of this paper.

We are grateful to ECMWF, the Climate and Global Dynamics Division of NCAR, and the Scientific Computing Division of NCAR for providing data, compositing software, and computing resources used in this study. This research was supported by the National Science Foundation through Grant ATM-9413012 and NOAA through Grant NA56GP0197, both awarded to SUNYA. The publication of this research was completed while the first author was a National Research Council Postdoctoral Research Associate at NSSL in Norman, Oklahoma.

REFERENCES

Aceituno, P., 1989: On the functioning of the Southern Oscillation in the South American sector. Part II: Upper-air circulation. *J. Climate*, **2,** 341–355.

Arkin, P. A., 1982: The relationship between interannual variability in the 200 mb tropical wind field and the Southern Oscillation. *Mon. Wea. Rev.*, **110,** 1393–1404.

Beebe, R. G., and F. C. Bates, 1955: A mechanism for assisting in the release of convective instability. *Mon. Wea. Rev.,* **83,** 1–10.

Bengtsson, L., M. Kanamitsu, P. Kållberg, and S. Uppala, 1982: FGGE 4-dimensional data assimilation at ECMWF. *Bull. Amer. Meteor. Soc.*, **63,** 29–43.

Bergeron, T., 1928: Über die dreidimensional verknüpfende Wetteranalyse, I. *Geofys. Publ.*, **5** (6), 1–111.

Bjerknes, J., 1969: Atmospheric teleconnections from the equatorial Pacific. *Mon. Wea. Rev.*, **97,** 163–172.

——, and H. Solberg, 1922: Life cycle of cyclones and the polar front theory of atmospheric circulation. *Geofys. Publ.*, **3** (1), 3–18.

Blackmon, M. L., 1976: A climatological spectral study of the 500 mb geopotential height of the Northern Hemisphere. *J. Atmos. Sci.*, **33,** 1607–1623.

Bosart, L. F., and B. E. Schwartz, 1979: Autumnal rainfall climatology of the Bahamas. *Mon. Wea. Rev.*, **107,** 1663–1672.

Boyle, J. S., 1986a: Comparison of the synoptic conditions in midlatitudes accompanying cold surges over eastern Asia for the

months of December 1974 and 1978. Part I: Monthly mean fields and individual events. *Mon. Wea. Rev.,* **114,** 903–918.
——, 1986b: Comparison of the synoptic conditions in midlatitudes accompanying cold surges over eastern Asia for the months of December 1974 and 1978. Part II: Relation of surge events to features of the longer term mean circulation. *Mon. Wea. Rev.,* **114,** 919–930.
——, and L. F. Bosart, 1983: A cyclone/anticyclone couplet over North America: An example of anticyclone evolution. *Mon. Wea. Rev.,* **111,** 1025–1045.
——, and T.-J. Chen, 1987: Synoptic aspects of the wintertime east Asian monsoon. *Monsoon Meteorology,* C.-P. Chang and T. N. Krishnamurti, Eds., Oxford University Press, 125–160.
Cavazos, T., and S. Hastenrath, 1990: Convection and rainfall over Mexico and their modulation by the Southern Oscillation. *J. Climatol.,* **10,** 377–386.
Chang, C.-P., and K. M. W. Lau, 1980: Northeasterly cold surges and near-equatorial disturbances over the winter MONEX area during December 1974. Part II: Planetary-scale aspects. *Mon. Wea. Rev.,* **108,** 298–312.
——, and ——, 1982: Short-term planetary-scale interactions over the Tropics and midlatitudes during northern winter. Part I: Contrasts between active and inactive periods. *Mon. Wea. Rev.,* **110,** 933–946.
——, and K. G. Lum, 1985: Tropical–midlatitude interactions over Asia and the western Pacific Ocean during the 1983/84 northern winter. *Mon. Wea. Rev.,* **113,** 1345–1358.
——, and J.-M. Chen, 1992: A statistical study of winter monsoon cold surges over the South China Sea and the large-scale equatorial divergence. *J. Meteor. Soc. Japan,* **70,** 287–302.
——, J. E. Erickson, and K. M. Lau, 1979: Northeasterly cold surges and near-equatorial disturbances over the winter MONEX area during December 1974. Part I: Synoptic aspects. *Mon. Wea. Rev.,* **107,** 812–829.
Chu, P.-S., 1988: Extratropical forcing and the burst of equatorial westerlies in the western Pacific: A synoptic study. *J. Meteor. Soc. Japan,* **66,** 549–564.
——, and S.-U. Park, 1984: Regional circulation characteristics associated with a cold surge event over east Asia during winter MONEX. *Mon. Wea. Rev.,* **112,** 955–965.
Colle, B. A., and C. F. Mass, 1995: The structure and evolution of cold surges east of the Rocky Mountains. *Mon. Wea. Rev.,* **123,** 2577–2610.
Colucci, S. J., and L. F. Bosart, 1979: Surface anticyclone behavior in NMC prediction models. *Mon. Wea. Rev.,* **107,** 377–394.
Crisp, C. A., and J. M. Lewis, 1992: Return flow in the Gulf of Mexico. Part I: A classificatory approach with a global historical perspective. *J. Appl. Meteor.,* **31,** 868–881.
Dallavalle, J. P., and L. F. Bosart, 1975: A synoptic investigation of anticyclogenesis accompanying North American polar air outbreaks. *Mon. Wea. Rev.,* **103,** 941–957.
Dickson, R. R., and J. Namias, 1976: North American influences on the circulation and climate of the North Atlantic sector. *Mon. Wea. Rev.,* **104,** 1255–1265.
DiMego, G. J., L. F. Bosart, and G. W. Endersen, 1976: An examination of the frequency and mean conditions surrounding frontal incursions into the Gulf of Mexico and Caribbean Sea. *Mon. Wea. Rev.,* **104,** 709–718.
Douglas, A. V., and P. J. Englehart, 1981: On a statistical relationship between autumn rainfall in the central equatorial Pacific and subsequent winter precipitation in Florida. *Mon. Wea. Rev.,* **109,** 2377–2382.
Enfield, D. B., 1996: Relationships of inter-American rainfall to tropical Atlantic and Pacific SST variability. *Geophys. Res. Lett.,* **23,** 3305–3308.
Estoque, M. A., J. Luque, M. Chandeck-Monteza, and J. Garcia, 1985: Effects of El Niño on Panama rainfall. *Geofis. Int.,* **24,** 355–381.
Frankenfield, H. C., 1917: ''Northers'' of the Canal Zone. *Mon. Wea. Rev.,* **45,** 546–550.
Garcia, I. P., 1996: Major cold air outbreaks affecting coffee and citrus plantations in the eastern and northeastern Mexico. *Atmósfera,* **9,** 47–68.
Gray, W. M., 1984: Atlantic seasonal hurricane frequency. Part I: El Niño and 30-mb quasi-biennial oscillation influences. *Mon. Wea. Rev.,* **112,** 1649–1668.
Grumm, R. H., and J. R. Gyakum, 1986: Systematic surface anticyclone errors in NMC's Limited Area Fine Mesh and spectral models during the winter of 1981/82. *Mon. Wea. Rev.,* **114,** 2329–2343.
Halpert, M. S., and C. F. Ropelewski, 1992: Surface temperature patterns associated with the Southern Oscillation. *J. Climate,* **5,** 577–593.
Hartjenstein, G., and R. Bleck, 1991: Factors affecting cold-air outbreaks east of the Rocky Mountains. *Mon. Wea. Rev.,* **119,** 2280–2292.
Hastenrath, S. L., 1967: Rainfall distribution and regime in Central America. *Arch. Meteor. Geophys. Bioklimatol. Ser. B,* **15,** 201–241.
——, L. C. de Castro, and P. Aceituno, 1987: The Southern Oscillation in the tropical Atlantic sector. *Beitr. Phys. Atmos.,* **60,** 447–463.
Henry, A. J., E. H. Bowie, H. J. Cox, and H. C. Frankenfield, 1916: *Weather Forecasting in the United States.* U.S. Government Printing Office, 370 pp.
Henry, W. K., 1979: Some aspects of the fate of cold fronts in the Gulf of Mexico. *Mon. Wea. Rev.,* **107,** 1078–1082.
Hill, J. B., 1969: Temperature variability and synoptic cold fronts in the winter climate of Mexico. Climatological Research Series, No. 4, McGill University, 71 pp. [Available from Dept. of Geography, McGill University, 805 Sherbrooke St. West, Montreal, PQ H3A 2K6, Canada.]
Horel, J. D., and J. M. Wallace, 1981: Planetary-scale atmospheric phenomena associated with the Southern Oscillation. *Mon. Wea. Rev.,* **109,** 813–829.
Horvath, N. C., and W. K. Henry, 1980: Some aspects of cold fronts in Belize. *Natl. Wea. Dig.,* **5** (4), 25–32.
Hoskins, B. J., I. N. James, and G. H. White, 1983: The shape, propagation and mean-flow interaction of large-scale weather systems. *J. Atmos. Sci.,* **40,** 1595–1612.
Hsu, H.-H., 1987: Propagation of low-level circulation features in the vicinity of mountain ranges. *Mon. Wea. Rev.,* **115,** 1864–1892.
Joung, C. H., and M. H. Hitchman, 1982: On the role of successive downstream development in East Asian polar air outbreaks. *Mon. Wea. Rev.,* **110,** 1224–1237.
Klaus, D., 1973: Las invasiones de aire frio en los tropicos a sotavento de las Montañas Rocallosas (Invasions of cold air in the Tropics on the lee side of the Rocky Mountains). *Geofis. Int.,* **13,** 99–143.
Klein, W. H., 1957: Principal tracks and mean frequencies of cyclones and anticyclones in the Northern Hemisphere. U.S. Weather Bureau Research Paper 40, 60 pp. [Available from Superintendent of Documents, U.S. Government Printing Office, Washington, DC 20225.]
Konrad, C. E., II, 1996: Relationships between the intensity of cold-air outbreaks and the evolution of synoptic and planetary-scale features over North America. *Mon. Wea. Rev.,* **124,** 1067–1083.
——, and S. J. Colucci, 1989: An examination of extreme cold air outbreaks over eastern North America. *Mon. Wea. Rev.,* **117,** 2687–2700.
Lackmann, G. M., L. F. Bosart, and D. Keyser, 1996: Planetary- and synoptic-scale characteristics of explosive wintertime cyclogenesis over the western North Atlantic Ocean. *Mon. Wea. Rev.,* **124,** 2672–2702.
Lau, K.-M., 1982: Equatorial response to northeasterly cold surges as inferred from satellite cloud imagery. *Mon. Wea. Rev.,* **110,** 1306–1313.
——, and P. H. Chan, 1983: Short-term climate variability and atmospheric teleconnections from satellite-observed outgoing longwave radiation. Part I: Simultaneous relationships. *J. Atmos. Sci.,* **40,** 2735–2750.
——, and C.-P. Chang, 1987: Planetary scale aspects of the winter

monsoon and atmospheric teleconnections. *Monsoon Meteorology*, C.-P. Chang and T. N. Krishnamurti, Eds., Oxford University Press, 161–202.

——, ——, and P. H. Chan, 1983: Short-term planetary-scale interactions over the tropics and midlatitudes. Part II: Winter-MONEX period. *Mon. Wea. Rev.*, **111,** 1372–1388.

Lau, N.-C., and K.-M. Lau, 1984: The structure and energetics of midlatitude disturbances accompanying cold-air outbreaks over east Asia. *Mon. Wea. Rev.*, **112,** 1309–1327.

Love, G., 1985: Cross-equatorial influence of winter hemisphere subtropical cold surges. *Mon. Wea. Rev.*, **113,** 1487–1498.

Mecikalski, J. R., and J. S. Tilley, 1992: Cold surges along the front range of the Rocky Mountains: Development of a classification scheme. *Meteor. Atmos. Phys.*, **48,** 249–271.

Mesinger, F., 1996: Forecasting cold surges east of the Rocky Mountains. Preprints, *15th Conf. on Weather Analysis and Forecasting*, Norfolk, VA, Amer. Meteor. Soc., 68–69.

Molinari, J., D. Knight, M. J. Dickinson, D. J. Vollaro, and S. T. Skubis, 1997: Potential vorticity, easterly waves, and eastern Pacific tropical cyclogenesis. *Mon. Wea. Rev.*, **125,** 2699–2708.

Orlanski, I., and J. P. Sheldon, 1995: Stages in the energetics of baroclinic systems. *Tellus*, **47A,** 605–628.

Panofsky, H. A., and G. W. Brier, 1968: *Some Applications of Statistics to Meteorology*. The Pennsylvania State University, 224 pp.

Ramage, C. S., 1968: Role of a tropical ''maritime continent'' in the atmospheric circulation. *Mon. Wea. Rev.*, **96,** 365–370.

Reding, P. J., 1992: The Central American cold surge: An observational analysis of the deep southward penetration of North American cold fronts. M.S. thesis, Department of Meteorology, Texas A&M University, 177 pp. [Available from Dept. of Meteorology, Texas A&M University, College Station, TX 77843-3150.]

Riehl, H., 1954: *Tropical Meteorology*. McGraw-Hill Book Company, 392 pp.

Rogers, J. C., 1988: Precipitation variability over the Caribbean and tropical Americas associated with the Southern Oscillation. *J. Climate*, **1,** 172–182.

——, and R. V. Rohli, 1991: Florida citrus freezes and polar anticyclones in the Great Plains. *J. Climate*, **4,** 1103–1113.

Ropelewski, C. F., and M. S. Halpert, 1987: Global and regional scale precipitation patterns associated with the El Niño/Southern Oscillation. *Mon. Wea. Rev.*, **115,** 1606–1626.

Saaroni, H., A. Bitan, P. Alpert, and B. Ziv, 1996: Continental polar outbreaks into the Levant and eastern Mediterranean. *J. Climatol.*, **16,** 1175–1191.

Schultz, D. M., W. E. Bracken, L. F. Bosart, G. J. Hakim, M. A. Bedrick, M. J. Dickinson, and K. R. Tyle, 1997: The 1993 superstorm cold surge: Frontal structure, gap flow, and tropical impact. *Mon. Wea. Rev.*, **125,** 5–39; Corrigendum, **125,** 662.

Schwartz, B. E., and M. Govett, 1992: A hydrostatically consistent North American radiosonde data base at the Forecast Systems Laboratory, 1946–present. NOAA Tech. Memo. ERL FSL-4, 81 pp. [Available from NOAA/ERL/FSL, 325 Broadway, Boulder, CO 80303.]

Simpson, J. E., 1987: *Gravity Currents: In the Environment and the Laboratory*. Ellis Horwood, 244 pp.

Steenburgh, W. J., and C. F. Mass, 1994: The structure and evolution of a simulated Rocky Mountain lee trough. *Mon. Wea. Rev.*, **122,** 2740–2761.

Stone, R. C., G. L. Hammer, and T. Marcussen, 1996: Prediction of global rainfall probabilities using phases of the Southern Oscillation index. *Nature*, **384,** 252–255.

Trasviña, A., E. D. Barton, J. Brown, H. S. Velez, P. M. Kosro, and R. L. Smith, 1995: Offshore wind forcing in the Gulf of Tehuantepec, Mexico: The asymmetric circulation. *J. Geophys. Res.*, **100,** 20 649–20 663.

Trenberth, K. E., 1992: Global analyses from ECMWF and atlas of 1000 to 10 mb circulation statistics. NCAR Tech. Note NCAR/TN-373+STR, 191 pp. [Available from NCAR Information Services, P. O. Box 3000, Boulder, CO 80307.]

——, and J. G. Olson, 1988: An evaluation and intercomparison of global analyses from the National Meteorological Center and the European Centre for Medium-Range Weather Forecasts. *Bull. Amer. Meteor. Soc.*, **69,** 1047–1057.

Uccellini, L. W., and D. R. Johnson, 1979: The coupling of upper and lower tropospheric jet streaks and implications for the development of severe convective storms. *Mon. Wea. Rev.*, **107,** 682–703.

Wallace, J. M., and D. S. Gutzler, 1981: Teleconnections in the geopotential height field during the Northern Hemisphere winter. *Mon. Wea. Rev.*, **109,** 784–812.

——, G.-H. Lim, and M. L. Blackmon, 1988: Relationship between cyclone tracks, anticyclone tracks and baroclinic waveguides. *J. Atmos. Sci.*, **45,** 439–462.

Waylen, P. R., M. E. Quesada, and C. N. Caviedes, 1994: The effects of El Niño–Southern Oscillation on precipitation in San José, Costa Rica. *J. Climatol.*, **14,** 559–568.

——, ——, and ——, 1996a: Temporal and spatial variability of annual precipitation in Costa Rica and the Southern Oscillation. *J. Climatol.*, **16,** 173–193.

——, C. N. Caviedes, and M. E. Quesada, 1996b: Interannual variability of monthly precipitation in Costa Rica. *J. Climate*, **9,** 2606–2613.

Webster, P. J., and J. R. Holton, 1982: Cross-equatorial response to middle-latitude forcing in a zonally varying basic state. *J. Atmos. Sci.*, **39,** 722–733.

Weiss, S. J., 1992: Some aspects of forecasting severe thunderstorms during cool-season return-flow episodes. *J. Appl. Meteor.*, **31,** 964–982.

Wu, M. C., and J. C. L. Chan, 1995: Surface features of winter monsoon surges over south China. *Mon. Wea. Rev.*, **123,** 662–680.

——, and ——, 1997: Upper-level features associated with winter monsoon surges over south China. *Mon. Wea. Rev.*, **125,** 317–340.

Wyrtki, K., 1975: El Niño—The dynamic response of the equatorial Pacific Ocean to atmospheric forcing. *J. Phys. Oceanogr.*, **5,** 572–584.

Yarnal, B., and H. F. Diaz, 1986: Relationships between extremes of the Southern Oscillation and the winter climate of the Anglo-American Pacific Coast. *J. Climatol.*, **6,** 197–219.